Molecular Therapy
Original Article

A single-shot adenoviral vaccine provides hemagglutinin stalk-mediated protection against heterosubtypic influenza challenge in mice

Carly M. Bliss,[1,9] Alec W. Freyn,[1,12] Tom G. Caniels,[1,10] Victor H. Leyva-Grado,[1,11] Raffael Nachbagauer,[1,13] Weina Sun,[1] Gene S. Tan,[2,3] Virginia L. Gillespie,[4] Meagan McMahon,[1] Florian Krammer,[1,5] Adrian V.S. Hill,[6] Peter Palese,[1] and Lynda Coughlan[1,7,8]

[1]Department of Microbiology, Icahn School of Medicine at Mount Sinai, One Gustave L. Levy Place, New York, NY 10029, USA; [2]Craig Venter Institute, La Jolla, CA 92037, USA; [3]Division of Infectious Disease, Department of Medicine, University of California, San Diego, La Jolla, CA 92037, USA; [4]The Center for Comparative Medicine and Surgery (CCMS) Comparative Pathology Laboratory, Icahn School of Medicine at Mount Sinai, New York, NY 10029, USA; [5]Department of Pathology, Icahn School of Medicine at Mount Sinai, New York, NY 10029, USA; [6]Jenner Institute, University of Oxford, Roosevelt Drive, Oxford OX3 7DQ, UK; [7]Department of Microbiology and Immunology, University of Maryland School of Medicine, Baltimore, MD 21201, USA; [8]Center for Vaccine Development and Global Health (CVD), University of Maryland School of Medicine, Baltimore, MD 21201, USA

Conventional influenza vaccines fail to confer broad protection against diverse influenza A viruses with pandemic potential. Efforts to develop a universal influenza virus vaccine include refocusing immunity towards the highly conserved stalk domain of the influenza virus surface glycoprotein, hemagglutinin (HA). We constructed a non-replicating adenoviral (Ad) vector, encoding a secreted form of H1 HA, to evaluate HA stalk-focused immunity. The Ad5_H1 vaccine was tested in mice for its ability to elicit broad, cross-reactive protection against homologous, heterologous, and heterosubtypic lethal challenge in a single-shot immunization regimen. Ad5_H1 elicited hemagglutination inhibition (HI^+) active antibodies (Abs), which conferred 100% sterilizing protection from homologous H1N1 challenge. Furthermore, Ad5_H1 rapidly induced H1-stalk-specific Abs with Fc-mediated effector function activity, in addition to stimulating both $CD4^+$ and $CD8^+$ stalk-specific T cell responses. This phenotype of immunity provided 100% protection from lethal challenge with a head-mismatched, reassortant influenza virus bearing a chimeric HA, cH6/1, in a stalk-mediated manner. Most importantly, 100% protection from mortality following lethal challenge with a heterosubtypic avian influenza virus, H5N1, was observed following a single immunization with Ad5_H1. In conclusion, Ad-based influenza vaccines can elicit significant breadth of protection in naive animals and could be considered for pandemic preparedness and stockpiling.

INTRODUCTION

Seasonal influenza virus epidemics cause significant annual mortality, estimated at 500,000–650,000 deaths worldwide. It has been >100 years since the 1918 H1N1 pandemic, which is believed to have resulted in the deaths of more than 40 million individuals.[1] Although subsequent pandemics (1957, 1968, and 2009) were less severe, there is an urgent need to develop a universal influenza vaccine capable of providing broad protection against seasonal and pandemic viruses.[2]

Neutralizing antibodies (NAbs) directed toward the head of the major surface glycoprotein, hemagglutinin (HA), can provide sterilizing protection against infection with influenza viruses. As such, HA is the main target for current seasonal influenza virus vaccines, including the inactivated influenza vaccine (IIV). There are currently 18 different influenza A virus (IAV) HA subtypes (H1–H18), which are phylogenetically subdivided into two main groups: group 1 (G1) and group 2 (G2).[3] The subtypes that circulate in humans and have caused pandemics in the past include H1, H2, and H3. However, there is ongoing concern that sporadic introduction of viruses bearing zoonotic HA subtypes (e.g., avian H5) into an immunologically naive human population could result in a severe pandemic.[2,4]

Received 20 August 2021; accepted 5 January 2022;
https://doi.org/10.1016/j.ymthe.2022.01.011.

[9]Present address: Division of Cancer & Genetics, Division of Infection & Immunity, School of Medicine, Cardiff University, Cardiff, Wales CF14 4XN, UK

[10]Present address: Department of Medical Microbiology, Amsterdam UMC, University of Amsterdam, Amsterdam Institute for Infection and Immunity, Meibergdreef 9, 1105 Amsterdam, the Netherlands

[11]Present address: Auro Vaccines, 401 N Middletown Road, Bldg 205, Third Floor, Pearl River, NY 10965, USA

[12]Present address: Moderna, Infectious Disease Research, Cambridge, MA 02139, USA

[13]Present address: Moderna, Infectious Disease Development, Cambridge, MA 02139, USA

Correspondence: Lynda Coughlan, PhD, Department of Microbiology and Immunology, Center for Vaccine Development and Global Health (CVD), University of Maryland School of Medicine, 685 W. Baltimore Street, HSF1, Office #380E, Baltimore, MD 21201, USA.
E-mail: lcoughlan@som.umaryland.edu

Please cite this article in press as: Bliss et al., A single-shot adenoviral vaccine provides hemagglutinin stalk-mediated protection against heterosubtypic influenza challenge in mice, Molecular Therapy (2022), https://doi.org/10.1016/j.ymthe.2022.01.011

HA is a homotrimeric protein composed of two domains, the receptor-binding head and a highly conserved stalk (or stem) domain. The globular head of HA is immunodominant but antigenically variable,[5] tolerating the accumulation of drift mutations. In contrast, the stalk is highly conserved antigenically but is immunosubdominant.[6] Following immunization with IIVs, the immunodominance of the HA head results in largely strain-specific humoral immune responses. As a result of the mutational plasticity of the HA head,[7–10] vaccine strains are often mismatched to circulating viruses, resulting in vaccine effectiveness as low as 10%.[11–15] Seasonal vaccine production is also hampered by the requirement to make advance predictions as to which influenza strains will circulate in the forthcoming influenza season. Another issue is that the manufacturing process is protracted, taking more than 6 months from strain identification to final delivery of the product.[2,16,17] Additional concerns include an over-reliance on eggs and the propensity for adaptation mutations arising from growth of vaccine strains in eggs, which negatively impacts vaccine effectiveness.[18–20] Consequently, the requirement for annual vaccine reformulation at a significant cost and issues associated with egg-based manufacturing support the urgent need to develop a universal influenza virus vaccine. To achieve this, efforts are focused on (1) increasing vaccine breadth by redirecting immunity toward highly conserved epitopes common to diverse influenza viruses and (2) investigating egg-independent vaccine platforms that could overcome some of the current vaccine limitations.

The high degree of intra-group similarity within the stalk domain of G1 HAs prompted efforts to refocus humoral immunity toward the stalk to elicit within-group, multi-subtype protection (e.g., H1 and H5). To date, pre-clinical studies have clearly demonstrated that sequential immunization (i.e., prime:boost) with novel immunogens, such as stabilized headless HAs[21–24] or chimeric HAs (cHAs),[25,26] can elicit broadly reactive antibodies (brAbs) against the stalk, which confer protection from heterosubtypic lethal challenge in animals. cHAs feature a conserved stalk domain grafted to the head of an exotic HA for which humans are naive (e.g., cH6/1)[27] and are compatible with IIV or live attenuated influenza vaccine (LAIV) platforms. Stalk-focused vaccines have advanced to clinical trials (NCT03300050, NCT03275389, and NCT03814720). In particular, the cHA approach demonstrated that stalk-reactive antibodies can be boosted in humans,[28,29] suggesting that universal protection could be achieved. In support of this, stalk-reactive antibodies have also been identified as an independent correlate of protection in a human cohort study of natural infection.[30]

To develop a vaccine platform that is completely independent of egg-based manufacturing, we engineered an adenoviral (Ad) vector encoding a secreted, trimeric H1 HA. We assessed its ability to elicit cross-reactive, stalk-mediated cellular and humoral immunity and protection in mice following a single shot, comparing it head to head with conventional IIV-based vaccines in homologous (H1), heterologous (cH6/1), and heterosubtypic (H5) lethal challenge models.

RESULTS

Validation of vaccine antigen expression and structural integrity *in vitro*

Inaccessibility or occlusion of stalk epitopes to B cell receptors by the HA head through shielding or steric hindrance, or as a result of membrane anchoring of HA on virions (such as on IIV), are mechanisms that have been proposed to explain the immunosubdominance of the HA stalk.[31] Therefore, we reasoned that expression of a secreted, trimeric form of H1 by a non-replicating Ad vector might maximize accessibility of cross-reactive stalk epitopes. First, we constructed a vaccine immunogen based on H1 (A/California/07/2009) in which the transmembrane domain was removed and replaced with a heterologous trimerization domain, fibritin foldon,[32] previously used to engineer soluble secreted HA[33] (Figure 1A). Prior to engineering an Ad5-based vaccine expressing H1, we confirmed that H1 was successfully secreted into the supernatant and that it was the correct size (Figure 1B). When purified, we verified that the H1 immunogen was structurally intact and recognized by monoclonal antibodies (mAbs) that bind conformation-sensitive epitopes on the HA stalk, including human mAbs CR9114[34] and FI6,[35] as well as murine mAbs KB2[27] and GG3[36] (Figures 1C and 1D). The H1 antigen was subsequently engineered into an Ad5-based vector, under the control of a cytomegalovirus (CMV) promoter to facilitate *in vivo* expression of secreted H1 from the Ad5_H1 vaccine construct following immunization of mice.

A single-shot of Ad5_H1 induces humoral immune responses that are superior to a traditional H1-matched inactivated influenza vaccine

Female BALB/cJ mice (n = 10/group) were vaccinated intramuscularly (i.m.) with Ad5_H1 at doses of 10^6, 10^7, or 10^8 infectious units (IFUs) at day 0 (D0) (Figure 1E). A positive control group consisted of matched H1 IIV administered at 1.5 μg of HA per dose. This dose represents $1/10^{th}$ the human dose and is a dose of IIV regularly used to confer sterilizing protection from homologous challenge in mice.[26] Mice in negative control groups were vaccinated with Ad5 encoding an irrelevant antigen, enhanced green fluorescent protein (EGFP) (Ad5_EGFP) at 10^8 IFUs, or with sterile PBS. Following a single vaccination, serum immunoglobulin G (IgG) antibody (Ab) responses were measured by enzyme-linked immunosorbent assay (ELISA) on D14 and D28 against full-length H1 protein, homologous to the H1 encoded by Ad5_H1 vaccine, and matched to the H1N1 IIV positive control (Figures 2A and 2B). Anti-H1 responses were detected at D14 and subsequently peaked at D28 in a dose-dependent manner (geometric mean endpoint titer 1.4×10^6 for 10^8, 6.4×10^5 for 10^7, and 2.5×10^5 for 10^6 IFUs Ad5_H1). More importantly, when compared with mice vaccinated with 1.5 μg of H1 IIV, D14 geometric mean endpoint titers were ~333-fold greater for 10^8 Ad5_H1 ($p = 0.0033$) and ~148-fold greater for 10^7 Ad5_H1 ($p = 0.0287$). At D28, Ab titers elicited by Ad5_H1 (10^8) were ~123-fold greater than those induced by H1N1 IIV ($p = 0.0019$). These data demonstrate that an Ad-based vaccine elicits rapid and strong Ab responses following a single immunization in mice, which is superior to serum IgG titers induced by a conventional, matched H1 IIV.

Please cite this article in press as: Bliss et al., A single-shot adenoviral vaccine provides hemagglutinin stalk-mediated protection against heterosubtypic influenza challenge in mice, Molecular Therapy (2022), https://doi.org/10.1016/j.ymthe.2022.01.011

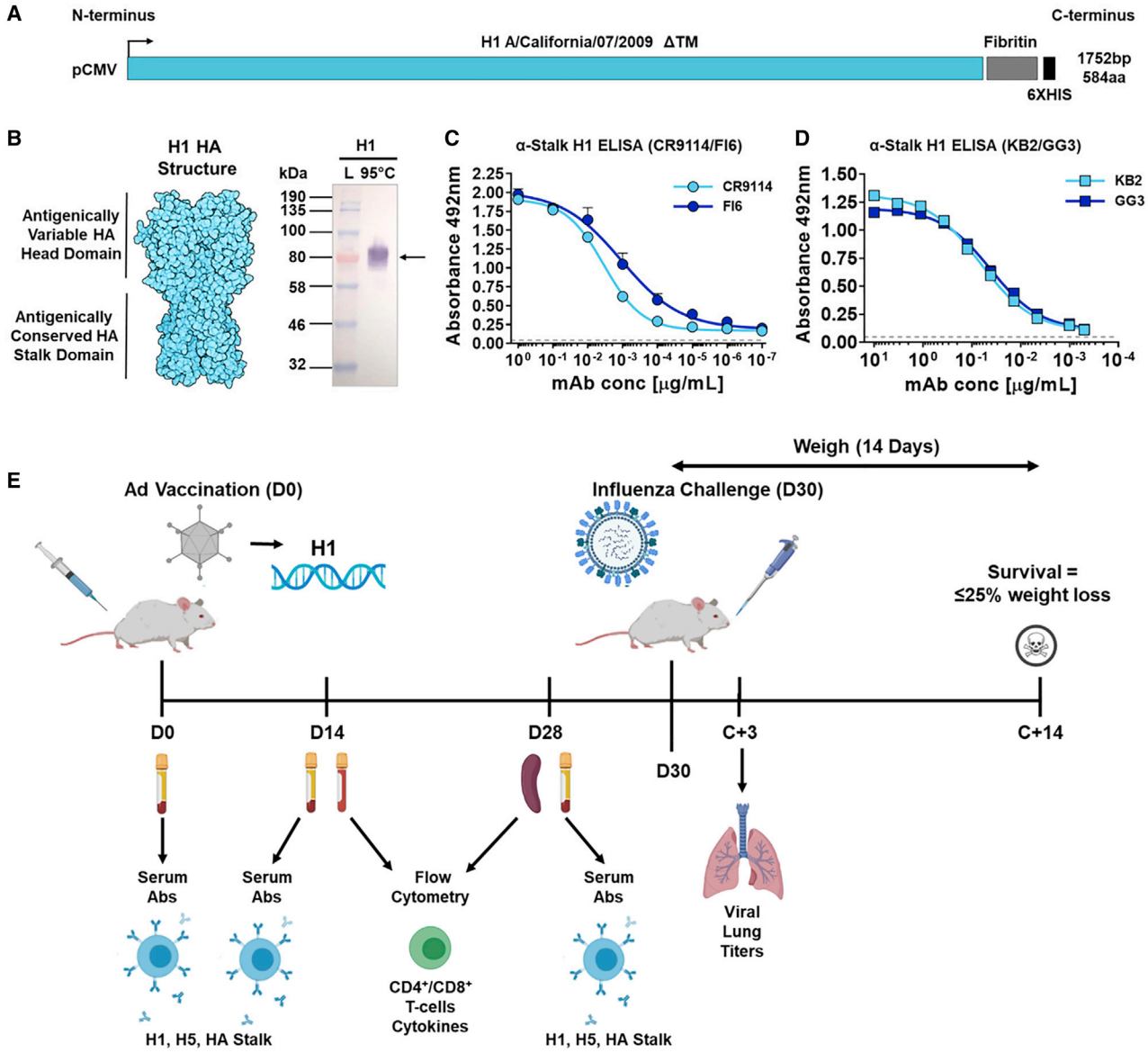

Figure 1. Adenoviral vaccine construction and schematic overview of mouse immunization and lethal challenge regimen

(A) A non-replicating adenoviral vector was engineered to encode influenza virus hemagglutinin (HA) subtype H1 (A/California/07/2009 H1), with antigen expression under the control of a CMV promoter. Vaccine antigen design involved deletion of the transmembrane domain (ΔTM) and the insertion of a heterologous trimerization domain (T4 foldon fibritin) and C-terminal 6XHIS tag. (B) Structure of a representative pandemic H1 immunogen (PDB: 4EDB), showing the HA head and stalk domain, as well as validation of H1 expression and multimerization as determined by western blot. (C and D) ELISA using monoclonal antibodies (mAbs) that recognize conformational epitopes on the HA stalk domain. Data points show mean ±SD. Dashed gray line in (C) and (D) shows a species-specific isotype control mAb used on every plate at the input concentration. (E) Schematic overview of vaccination and bleed schedule of mice, prior to influenza virus challenge. Mice received a single intramuscular (i.m.) vaccination on day 0 (D0) with blood sampling at baseline, D14, and/or D28 for measuring immunogenicity, followed by intranasal (i.n.) influenza virus challenge at D30 and lung dissection for lung viral titers on a subset of mice (n = 3) at D33 (C+3). Infected mice were monitored daily for weight loss and survival in the 2 weeks following challenge (C+14). 6XHIS, 6X histidine tag; Abs, antibodies; Ad, adenovirus; CMV, cytomegalovirus; ELISA, enzyme-linked immunosorbent assay; HA, hemagglutinin; kDa, kilodalton; L, ladder; mAb, monoclonal antibody.

An established absolute correlate of protection for influenza virus vaccines is an Ab hemagglutination inhibition (HI) titer of 1:40.[37–39] Strain-matched, head-specific Abs with HI activity can confer sterilizing immunity and protection from homologous challenge. Therefore, we assessed the ability of Ad5_H1 to induce HI active Abs when compared with a matched H1N1 IIV (Figure 2C). Following a single shot of Ad5_H1, HI^+ Ab titers in mouse serum against pH1N1 virus increased in a dose-dependent manner, with

Please cite this article in press as: Bliss et al., A single-shot adenoviral vaccine provides hemagglutinin stalk-mediated protection against heterosubtypic influenza challenge in mice, Molecular Therapy (2022), https://doi.org/10.1016/j.ymthe.2022.01.011

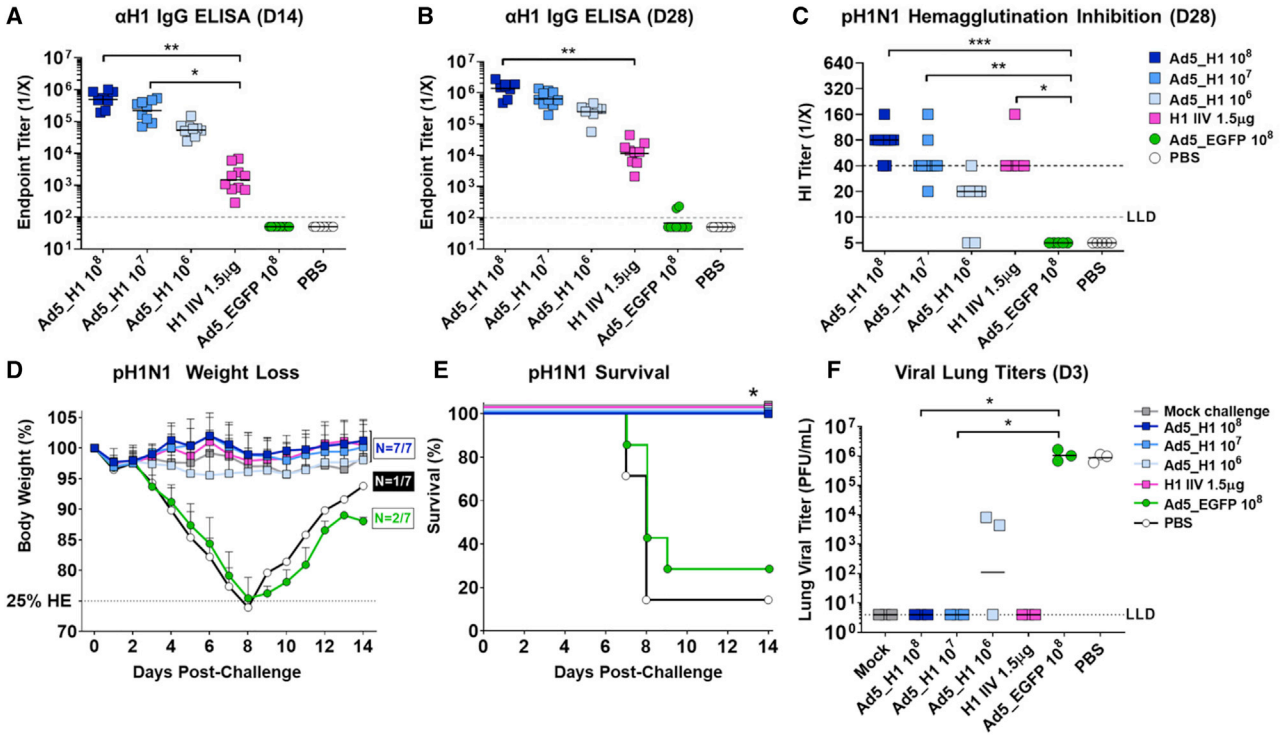

Figure 2. A single shot of Ad5_H1 confers superior protection to an H1-matched inactivated influenza vaccine (IIV) following homologous lethal pH1N1 influenza virus challenge

BALB/cJ female mice were immunized i.m. with a single shot of Ad5_H1 (A/California/07/2009) at doses of 10^8–10^6 infectious units (IFUs), a matched monovalent split-virion H1N1 IIV (BEI no. NR-20347) at 1.5 μg, or Ad5_EGFP, an irrelevant antigen control at 10^8 IFUs. (A–C) Humoral immune responses were measured at D14 or D28 post-immunization by (A and B) serum IgG ELISA against full-length recombinant H1 (A/California/07/2009; BEI no. NR-44074) and (C) hemagglutination inhibition (HI) assay against pH1N1 virus. For ELISA titers, the line on data points indicates the geometric mean, and the dashed gray line in (A) and (B) indicates the input serum dilution and represents the lower limit of detection (LLD). The line on data points in the HI assay (C) denotes median. The dashed black line in (C) indicates an HI titer ≥1:40, which is a correlate of protection in humans. (D–F) At D30 post-immunization, mice were challenged i.n. with 5× mLD50 (300 PFUs) wild-type pH1N1 diluted in sterile PBS (50 μL). Vaccine efficacy was assessed by measuring morbidity (weight loss), mortality (survival), and lung viral titers on D3 post-challenge (C+3). (D) Weight loss data show mean and SD. The humane endpoint was reached when mice lost 25% body weight. (F) For lung viral titers, the line on data points indicates the geometric mean and dashed line indicates the LLD (minimum of one plaque counted × dilution factor). Statistical analyses were performed using the Kruskal-Wallis test with Dunn's correction for multiple comparisons against the H1N1 IIV vaccine or against irrelevant vaccine, Ad5_EGFP. *$p < 0.05$, **$p < 0.01$, and ***$p < 0.001$. Survival significance thresholds were calculated using log rank (Mantel-Cox test), corrected for multiple comparisons against Ad5_EGFP using Bonferroni method with K = 4, *$p < 0.05$.

100% of mice that received Ad5_H1 10^8 IFUs exhibiting an HI titer of ≥1:40, with a median titer of 1:80. Vaccination with Ad5_H1 at 10^7 IFUs induced HI^+ Abs with a median titer of 1:40 and resulted in HI activity in 100% of mice. At the lowest dose of Ad5_H1 (10^6), vaccination induced HI active Abs in the serum of 70% of mice, with a median titer of 1:20. A single dose of H1N1 IIV administered i.m. elicited an HI of ≥1:40, while no HI titer activity was induced by negative control vaccines Ad5_EGFP or PBS.

A single shot of Ad5_H1 confers superior protection to an H1-matched IIV following homologous pH1N1 lethal influenza virus challenge

To determine the protective efficacy of Ad5_H1 vaccine, we designed a challenge experiment to evaluate homologous (matched H1) protection following a single immunization (Figure 1E). Efficacy following homologous influenza virus challenge was assessed using three measures: (1) weight loss; (2) survival; and (3) viral lung titers. Mice were challenged with five times the median mouse lethal dose (mLD_{50}) of wild-type pH1N1 influenza virus (A/Netherlands/602/2009). Following pH1N1 challenge, <6% mean weight loss was measured in all Ad5_H1-vaccinated groups (10^6–10^8 IFUs), comparable to mice vaccinated with a matched H1 IIV, a positive control for protection in this challenge model (Figure 2D). Survival after pH1N1 challenge was significantly higher in Ad5_H1 (100%) and H1 IIV groups (100%) when compared with mice vaccinated with Ad5_EGFP (~28%) or unvaccinated PBS control animals (~14%; Figure 2E). Vaccinated mice with median HI titer of ≥1:40 against pH1N1 had complete sterilizing protection, with no virus detected in the lungs at D3 following challenge (C+3) with pH1N1 (Figure 2F). Consistent with the dose-dependent effect of Ad5_H1 on HI^+ Abs (Figure 2C), 2/3 mice that received the lowest dose of Ad5_H1 (10^6 IFUs) lacked complete sterilizing immunity,

Please cite this article in press as: Bliss et al., A single-shot adenoviral vaccine provides hemagglutinin stalk-mediated protection against heterosubtypic influenza challenge in mice, Molecular Therapy (2022), https://doi.org/10.1016/j.ymthe.2022.01.011

with virus titers of $\sim 10^4$ plaque-forming units (PFUs)/mL detected in the lungs on D3 post-challenge (Figure 2F).

Immunization with Ad5_H1, but not IIV-based vaccines, elicits H1-stalk-specific T cell responses

In contrast to strain-specific immune responses, which are largely directed toward the immunodominant HA head, stalk-specific immunity can be broadly cross-reactive. It would therefore be desirable for a universal influenza vaccine candidate to elicit stalk-reactive immunity. It has been observed that IIV platforms do not elicit robust stalk responses following a single shot and are limited in their ability to induce robust T cell responses.[40–44] In contrast, Ad vaccines are known to be potent inducers of cellular immunity, particularly $CD8^+$ T cells.[45–50] Therefore, to provide foundations for subsequent cH6/1N5 or H5N1 challenge experiments in which stalk immunity would be relevant to protection, we quantified stalk-specific T cell responses elicited following immunization with Ad5_H1 when compared with IIV or irrelevant antigen controls.

Flow cytometry with intracellular cytokine staining (ICS) was performed on peripheral blood mononuclear cells (PBMCs) on D14 or splenocytes on D28, which were stimulated with overlapping peptides corresponding to the H1 stalk (Table S1). Preliminary studies comparing Ad5_H1 with IIVs demonstrated that immunization with a single shot of IIV (H1N1 or H5N1) did not elicit detectable stalk-specific T cells in peripheral blood (Figure S1). Therefore, the IIV groups were not included in subsequent ICS analyses. In contrast, we detected robust T cell responses to immunization with all doses of Ad5_H1. ICS performed on splenocytes demonstrated that the interferon γ (IFN-γ) H1-stalk-specific response consisted of both $CD4^+$ and $CD8^+$ T cells (Figures 3A and 3E). The $CD4^+$ T cell response against the H1 stalk was a low-frequency T helper 1 phenotype, with statistically significant frequencies of $CD4^+$ T cells expressing pro-inflammatory cytokines IFN-γ (geometric mean frequency of 0.03%), interleukin-2 (IL-2) (0.05%), and tumor necrosis factor alpha (TNF-α) (0.05%) following immunization with Ad5_H1 compared with Ad5_EGFP control mice (Figures 3A–3C). $CD4^+$ T cells also upregulated intracellular CD40 ligand (CD40L/CD154; 0.04%; Figure 3D), which is expressed on the surface of activated T cells and plays a role in providing T cell help to B cells.[51]

In agreement with published studies for Ad5-based vaccines, $CD8^+$ responses were of higher magnitude than $CD4^+$ T cell responses,[45–47,52] and higher frequencies of cells secreting pro-inflammatory cytokines IFN-γ (geometric mean frequency of 0.60%), IL-2 (0.12%), and TNF-α (0.48%) were detected in Ad5_H1 immunized mice than in Ad5_EGFP control mice (Figures 3E–3G). H1-stalk-specific induction of degranulation marker CD107a (0.48%) in $CD8^+$ T cells suggested that these cells also had cytotoxic potential (Figure 3H). H1-stalk-specific $CD8^+$ T cell responses following immunization with Ad5_H1 were also detectable in the peripheral blood at D28: IFN-γ (0.69%); IL-2 (0.07%); TNF-α (0.36%); and CD107a (0.56%). As stated above, no stalk-reactive T cell responses were measured in peripheral blood following immunization with IIV (Figures S1A–S1D). The phenotype of the H1-stalk-specific response was further characterized through the degree of $CD4^+$ and $CD8^+$ T cell polyfunctionality. The $CD4^+$ splenocyte response was highly polyfunctional, with dominant populations of $CD40L^+$ IFN-γ^+ IL-2^+ TNF-α^+ and $CD40L^+$ IFN-γ^- IL-2^+ TNF-α^+ (Figure 3I). The dominant $CD8^+$ splenocyte T cell population was also highly polyfunctional, with CD107a expression, IFN-γ, and TNF-α production in an Ad5_H1 dose-dependent manner (Figure 3J).

A single-shot of Ad5_H1, but not traditional IIV vaccines, elicits HA-stalk-specific Abs with Fc-effector function activity

A long-standing goal in the development of a universal influenza virus vaccine is to elicit cross-reactive, stalk-specific humoral immunity that can confer broad protection from heterologous or heterosubtypic viruses, independently of strain-specific head Abs. With this in mind, it is important to note that the mechanism of protection conferred by broadly reactive, stalk-focused immunity is completely distinct from classical hemagglutination inhibiting HI^+, head-specific NAbs, which provide sterilizing immunity through prevention of virus binding and/or viral entry. Although stalk-specific Abs *can* have neutralizing activity, many brAbs are non-neutralizing *in vitro* but can protect *in vivo* through engagement of Fc-mediated effector functions, such as Ab-dependent cellular cytotoxicity (ADCC).[53–56] Stalk-specific Abs do not generally confer sterilizing protection from infection in the lung[56–60] but, importantly, can confer broad protection from lethal challenge.

To determine whether Ad5_H1 could induce stalk-specific Abs following a single immunization, female BALB/cJ mice (n = 10/group) were vaccinated i.m. as before (Figure 1E). As these studies were performed in preparation for a challenge to measure stalk-based protection (using a chimeric cH6/1 challenge), as well as a subsequent heterosubtypic H5N1 lethal challenge, we included sera from H1 IIV and H5 IIV-immunized mice to determine whether these vaccines could induce stalk-reactive Abs (Figures 4A and 4B). Negative controls were vaccinated with Ad5_EGFP at 10^8 IFUs or with PBS.

To measure stalk Abs, we produced and validated recombinant headless, trimeric H1 protein, based on the MiniHA #4900 construct previously described by Impagliazzo et al.[23] (Figures S2A and S2B). Total IgG against MiniHA (H1 stalk) was measured by ELISA. Vaccination with Ad5_H1 10^8 and 10^7 IFUs rapidly induced anti-H1 stalk IgG by D14. At D28, all three doses of Ad5_H1 vaccine induced statistically significant titers of anti-H1 stalk Abs (geometric mean endpoint titers were 1.2×10^4 for 10^8, 1.1×10^4 for 10^7, and 2.2×10^3 for 10^6 IFU Ad5_H1) as compared with the stalk-matched H1 IIV control vaccine. At both time points, anti-H1 stalk Ab titers were comparable between the Ad5_H1 10^8 and 10^7 IFUs dose. There was no induction of anti-H1 stalk Abs following immunization with H1- or H5-IIV (Figures 4A and 4B). As we detected the presence of stalk-reactive Abs, we also tested their potential for stalk-mediated neutralization of a cH6/1 reassortant virus that bears the H1 stalk matched to our vaccine immunogen (A/California/07/2009) and an irrelevant head (H6

Please cite this article in press as: Bliss et al., A single-shot adenoviral vaccine provides hemagglutinin stalk-mediated protection against heterosubtypic influenza challenge in mice, Molecular Therapy (2022), https://doi.org/10.1016/j.ymthe.2022.01.011

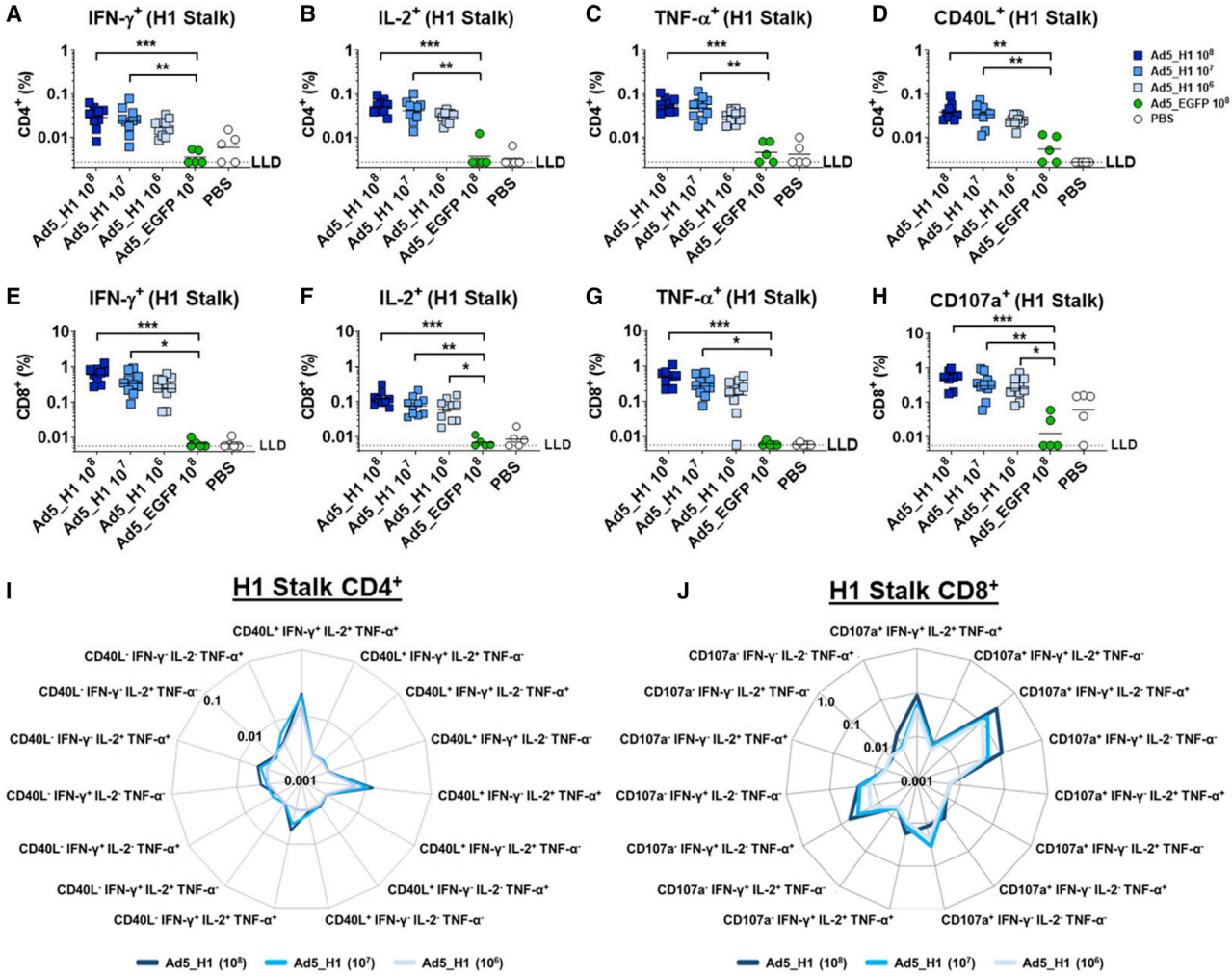

Figure 3. H1-stalk-specific T cell responses in the spleen 28 days post-vaccination

(A–H) Intracellular cytokine staining for (A–D) IFN-γ^+, IL-2^+, TNF-α^+, or CD40L$^+$ CD4^+ T cells and (E–H) IFN-γ^+, IL-2^+, TNF-α^+, or CD107a$^+$ CD8^+ T cells following H1 stalk peptide stimulation (see Table S1). Line indicates geometric mean, based on frequencies of cytokine-positive cells as a proportion of the parent CD4^+ or CD8^+ T cell population. Statistics were performed using the Kruskal-Wallis test with Dunn's correction for multiple comparisons against the Ad5_EGFP control group; *$p < 0.05$, **$p < 0.01$, and ***$p < 0.001$. Dashed line indicates the LLD of the assay. (I and J) Radar plots show polyfunctionality of the (I) H1-stalk-specific CD4^+ T cell response or the (J) H1-stalk-specific CD8^+ T cell response. Geometric mean frequencies are displayed.

from A/mallard/Sweden/81/2002). However, microneutralization (MN) assays against the cH6/1N5 virus did not detect NAbs above control groups for any of the vaccination regimens tested (Figure S3A).

Cross-reactive stalk Abs have been shown to confer protection *in vivo* through non-neutralizing, Fc-mediated effector functions, such as ADCC.[54,56,61,62] Therefore, using a luciferase-based reporter assay, we measured the amount of ADCC active Abs in pooled sera of mice vaccinated with Ad5_H1, H1- and H5-IIV, and Ad5_EGFP/PBS controls (Figure 4C). This assay was performed using a Madin-Darby canine kidney (MDCK) stable cell line expressing the cH6/1 on the cell surface.[63] HA expression in this cell line or in influenza-virus-infected cells was confirmed prior to the assay using mAbs against the HA stalk (Figures S4A–S4H). The ability of post-vaccination serum to bind the HA stalk and concomitantly activate Jurkat cells expressing murine Fcγ-receptor IV (FcγRIV) through engagement via the Fc domain:FcγRIV results in expression of luciferase (Figures S4I and S4J). Area under the curve (AUC) analysis of relative light units revealed FcγRIV activation when testing sera from all Ad5_H1-vaccinated groups but no activation when using serum from mice vaccinated with H1 IIV, H5 IIV, Ad5_EGFP, or PBS (Figure 4C). The ADCC reporter assay was also performed using Ad5_H1 serum on wild-type MDCK cells that do not express cH6/1, and no increase in FcγRIV activation was measured (Figures S4K and S4L). In summary, these data confirmed FcγRIV engagement and activation by immune sera from

Please cite this article in press as: Bliss et al., A single-shot adenoviral vaccine provides hemagglutinin stalk-mediated protection against heterosubtypic influenza challenge in mice, Molecular Therapy (2022), https://doi.org/10.1016/j.ymthe.2022.01.011

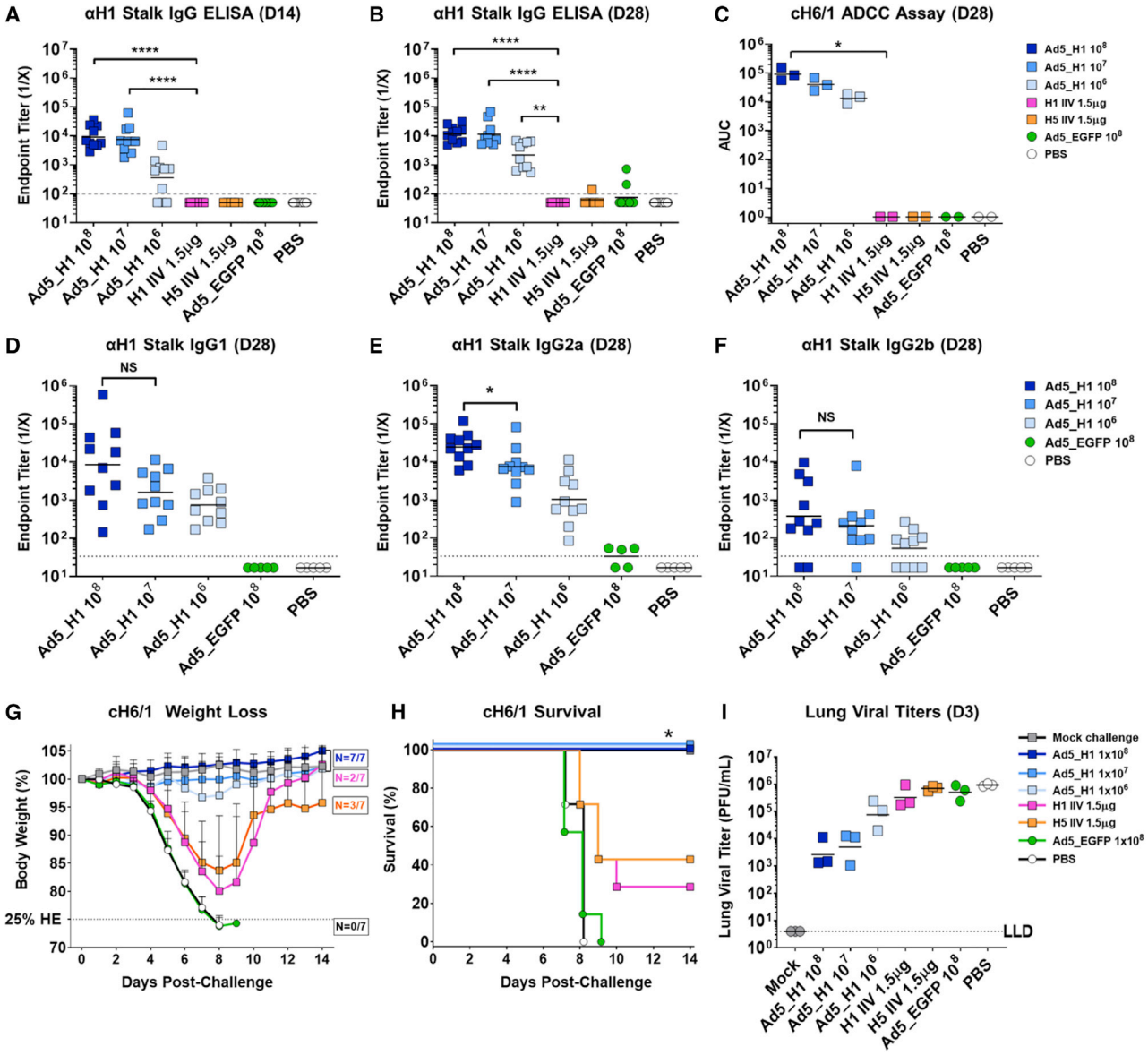

Figure 4. A single shot of Ad5_H1 confers 100% HA stalk-mediated protection from lethal challenge, which is superior to conventional H1N1 and H5N1 inactivated influenza vaccines (IIVs)

BALB/cJ female mice were immunized i.m. with a single shot of Ad5_H1 (A/California/07/2009) at doses of 10^8–10^6 IFUs, a matched monovalent split virion H1N1 IIV (BEI no. NR-20347) at 1.5 μg, an unadjuvanted H5N1 whole virion IIV (BEI no. NR-12147) at 1.5 μg, or Ad5_EGFP, an irrelevant antigen control at 10^8 IFUs. (A–C) HA-stalk-specific antibodies were measured at D14 or D28 by (A and B) serum IgG ELISA against headless H1 protein (MiniHA) and (C) using a reporter-based assay to measure antibody-dependent cellular cytotoxicity (ADCC) against the H1 stalk of MDCK cells stably expressing chimeric HA, cH6/1. For the ADCC assay, data points represent pooled sera (n = 5 mice), with each replicate derived from a separate immunization experiment. Statistical analyses were performed using the Kruskal-Wallis test with Dunn's correction for multiple comparisons against the H1N1 IIV vaccine. *$p < 0.05$, **$p < 0.01$, and ****$p < 0.0001$. (D–F) Stalk-specific antibody isotype subclass responses were measured against MiniHA headless H1. Statistical analyses were performed using the Mann-Whitney test comparing a dose of 10^8 Ad5_H1 with a dose of 10^7 IFUs. *$p < 0.05$; NS, not significant. (G–I) At D30 post-immunization, mice were challenged i.n. with 10× mLD50 cH6/1N5 diluted in sterile PBS (50 μL). The cHA challenge virus, cH6/1, has the stalk of H1 A/California/04/2009 grafted to the head of H6 A/mallard/Sweden/81/2002. Vaccine efficacy was assessed by measuring (G) morbidity (weight loss), (H) mortality (survival), and (I) lung viral titers at D3 post-challenge (C+3). The humane endpoint was reached when mice lost 25% body weight. Weight loss data show mean and SD. The line on data points for ELISA and lung titers indicates the geometric mean, and the dashed gray line indicates the LLD. For lung titers, this represents a minimum of one plaque counted × dilution factor. Survival significance thresholds for Ad5_H1 (10^8–10^6 IFUs) were calculated using log rank (Mantel-Cox test), corrected for multiple comparisons comparing Ad5_H1 (10^8–10^6) against H1 IIV using Bonferroni method with K = 3 and *$p < 0.05$.

mice vaccinated with all doses of Ad5_H1, but not with H1 IIV, H5 IIV, or negative control vaccines Ad5_EGFP or PBS (Figure 4C).

It is well established that the isotype or IgG subclass of Ab can differentially affect the activation of FcγRs. Mouse IgG2a and IgG2b antibodies bind activating mouse FcγRI and FcγRIV with high affinity (in mice, the hierarchy is IgG2a > IgG2b > IgG1).[64,65] Therefore, determining the IgG subclass of the stalk-reactive immune response elicited by vaccination is informative, as these classes of Abs differentially engage with activating FcγRs on the surface of diverse effector cells *in vivo* and could have an impact on protection. To investigate whether this was consistent with our ADCC data (Figure 4C), further characterization of the cross-reactive stalk Ab response was performed to identify the subclass of anti-stalk IgG induced (Figures 4D–4F). As no stalk Abs were induced following immunization with the H1 IIV or H5 IIV, these groups were not included in the analysis. Sera from Ad5_EGFP and PBS groups were included as negative controls. Following Ad5_H1 vaccination, the dominant IgG subclass detected was IgG2a > IgG1 > IgG2b, consistent with a prior study.[46] No significant difference was observed between the 10^8 and 10^7 Ad5_H1 doses for stalk-specific IgG1 (Figure 4D). However, endpoint titers of IgG2a antibodies against the MiniHA H1 stalk were induced in a dose-dependent manner, with responses ∼3.3-fold higher following Ad5_H1 vaccination at 10^8 IFUs compared with 10^7 or ∼24-fold higher when compared with a dose of 10^6 IFUs (Figure 4E). IgG2b induction was low across all Ad5_H1 groups, although slight differences were observed between 10^8 and 10^6 Ad5_H1 groups (Figure 4F).

A single shot of Ad5_H1 confers 100% HA stalk-mediated protection from chimeric cH6/1N5 lethal challenge in the absence of matched head-specific immunity

We established that a single-shot immunization with Ad5_H1 can elicit H1-stalk-reactive T cell responses and stalk-specific Abs that exhibit Fc-mediated effector function using an *in vitro* reporter assay. Therefore, we wanted to evaluate whether this phenotype of immune response could provide protection *in vivo*, in the absence of head-specific HI^+ Abs. Vaccine efficacy following influenza virus challenge was assessed using three measures: (1) weight loss; (2) survival; and (3) viral lung titers. Mice were challenged with 10× mLD_{50} of a cH6/1N5 reassortant virus bearing a chimeric H6/1 HA. The HA stalk of the cH6/1N5 virus is homologous to the H1 encoded in the Ad5_H1 vaccine, but the head is mismatched and derived from H6 A/mallard/Sweden/81/2002. To negate any confounding results with anti-N1 antibodies induced by the H1N1/H5N1 IIVs, the cH6/1N5 virus bears an avian N5 from A/mallard/Sweden/86/2003 and all other internal proteins from A/Puerto Rico/08/1934.[58]

Similar to the results obtained in the homologous pH1N1 challenge (Figure 2D), weight loss was minimal (<5%) in all Ad5_H1-vaccinated groups (10^6–10^8 IFUs), whereas humane endpoints were reached in negative control groups (Ad5_EGFP and PBS), and there was substantial weight loss in mice vaccinated with conventional H1 IIV or H5-IIV-based vaccines (Figure 4G). Protection against mortality (survival) was statistically significant in all Ad5_H1 groups (100%) when compared with H1 IIV (Figure 4H). All mice vaccinated with Ad5_EGFP or PBS reached the humane weight loss endpoint by D9 (Figure 4H). Although not found to be statistically significant, viral lung titers were also substantially reduced in animals immunized with Ad5_H1, with ∼335-fold, ∼174-fold, and ∼11-fold reductions for doses of 10^8–10^6, respectively, as compared with PBS (Figure 4I).

Ab binding to the HA stalk and triggering Fc-mediated effector functions through FcγR activation has the potential to protect against influenza virus challenge *in vivo*, through the induction of ADCC.[54,55] In support of this, the dose-dependent FcγRIV activation we previously measured in sera from Ad5_H1-vaccinated mice (see Figure 4C) is consistent with a non-significant yet substantial reduction in lung viral titers on D3 post-challenge with H1 stalk-matched cH6/1N5 virus (Figure 4I). The ADCC data also align with increased titers of stalk-specific Abs of the IgG2a isotype in mice immunized with Ad5_H1 (see Figure 4E). In addition, it is clear that conventional IIV-based vaccines, which did not elicit detectable stalk Abs, fail to reduce viral lung titers following challenge with a mismatched heterologous virus. Despite the stalk of H1 IIV being matched to the H1 stalk of the cH6/1N5 challenge virus, the H1 IIV provided no protection from lung infection, with high titers of virus in the lungs that were comparable to lung titers in mice immunized with PBS/Ad5_EGFP.

For pathological evaluation, lung tissue was harvested from a subset of animals that reached humane endpoints on D7–D10 post-challenge (i.e., H1- and H5-IIV-, Ad5_EGFP-, and PBS-vaccinated mice). Similar samples were taken from surviving animals at D14 post-challenge upon termination of the experiment, including H1 IIV (n = 2), H5 IIV (n = 2), PBS "mock" challenged mice, and all doses of Ad5_H1 (n = 3/group). Tissue was embedded in paraffin and sections stained with hematoxylin and eosin (H&E). A veterinary pathologist blinded to treatment groups, with the exception of the PBS-vaccinated + cH6/1 challenge and PBS mock challenge group, scored and imaged the sections (Figures 5A and 5B). A composite pathological score out of a total of 36 (see details in Supplemental Methods) is shown in Figure S5A. As expected, overall scores following euthanasia on D7–D10 for PBS-vaccinated (16/36) and Ad5_EGFP- (14/36) and H1- and H5-IIV-immunized animals (20/36) were relatively similar and were substantially higher than PBS mock-challenged control sections (3/36). Upon termination of the experiment at D14, scores for Ad5_H1 at doses of 10^8 (6/36) and 10^7 (7/36) were low, suggesting that immunization with Ad5_H1 resulted in increased protection from lung damage. Scores for Ad5_H1 at 10^6 IFUs (14/36) were comparable to the small numbers of surviving mice from the H1 IIV (n = 2) and H5 IIV groups (n = 2).

Overall, at D7–D10 post-challenge, inflammation affecting the alveoli was predominantly neutrophilic, mixed with lesser numbers of lymphocytes, plasma cells, and macrophages (Figure 5A). Inflammation of the bronchi and bronchioles was also neutrophilic, mixed with lymphocytes, though lesser numbers of plasma cells and macrophages were observed. Perivascular inflammation was also noted and was composed

Please cite this article in press as: Bliss et al., A single-shot adenoviral vaccine provides hemagglutinin stalk-mediated protection against heterosubtypic influenza challenge in mice, Molecular Therapy (2022), https://doi.org/10.1016/j.ymthe.2022.01.011

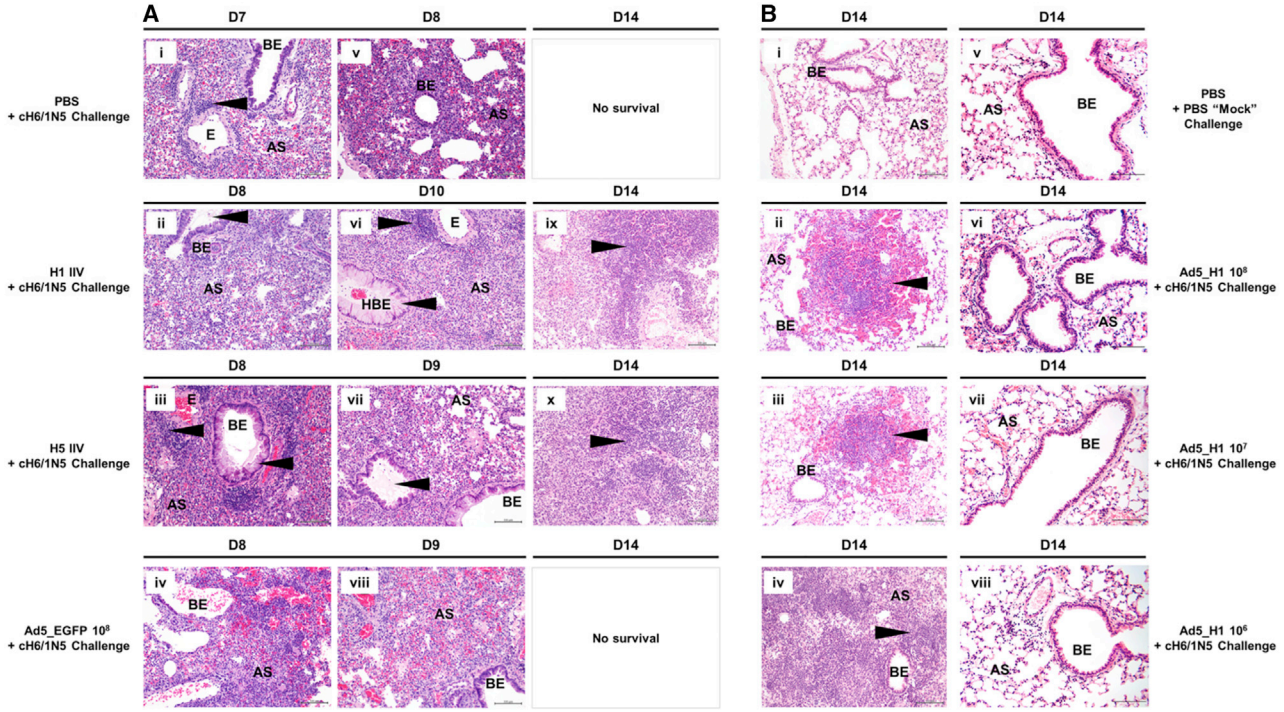

Figure 5. Hematoxylin and eosin (H&E) staining of murine lung sections following challenge with cH6/1N5 virus

BALB/cJ female mice were challenged i.n. with cH6/1N5 virus at D30 following i.m. immunization with (A) PBS, an H1 or H5 IIV at 1.5 μg, or Ad5_EGFP at 1×10^8 IFUs or with (B) Ad5_H1 at doses of 1×10^8–1×10^6 IFUs. Control groups were mock challenged with PBS. Lungs were harvested when animals reached the humane endpoint (≤25% body weight loss). For groups where survival was 100% (shown in B), lungs were harvested upon termination of the experiment at D14 post-challenge (n = 3/group). Lungs were inflated with 10% formalin, fixed and processed for paraffin embedding, and 5-μm sections stained for H&E. Lung anatomical regions are indicated on sections; AS, alveolar septa; BE, bronchiolar epithelium; E, endothelium. Arrows indicate histological observations, including perivascular inflammation (Ai, Aiii, and Avi), goblet cell hyperplasia (Aiii and Avi), intraluminal debris (Aii, Aiii, and Avii), or the formation of clusters of lymphocytes and plasma cells (Aix, Ax, Bii, and Biii). Sections shown were selected on the basis of a score closest to the average pathological score (Figure S5A), as determined by a veterinary pathologist blinded to the vaccine treatment groups. Images were captured using an Olympus BX43 and an Olympus DP21 Digital Camera system under 200× magnification. Scale bars represent 100 μm.

of lymphocytes and plasma cells. The lungs of mice immunized with PBS, H1/H5 IIV, or Ad5_EGFP had large areas of consolidation, where alveolar spaces were completely effaced by inflammatory infiltration and/or pneumocyte hyperplasia, with loss of septal architecture. Of note, a mix of proteinaceous fluid and cells, as well as intraluminal debris, was observed in the lungs of H1- and H5-IIV-vaccinated animals (i.e., Figures 5Aii and 5Avii). In addition, these mice had increased numbers of goblet cells. When compared with PBS mock challenge mice, the lungs of unvaccinated + cH6/1N5 animals, as well as mice immunized with H1/H5 IIV or Ad5_EGFP, had significant cellular inflammation (Figure 5A). For high doses of Ad5_H1 (10^8 and 10^7) on D14, there was minimal lymphoplasmacytic inflammation (0%–25% lung affected), but this was increased (25%–50% lung affected) in the lungs of challenged mice immunized with Ad5_H1 at 10^6 IFUs, although some areas of the lung were also unaffected (Figure 5B). Overall, these data demonstrate that, in the absence of head-specific Abs, a single immunization with high-dose Ad5_H1 can provide stalk-mediated protection from lung infection and damage. This represents an advance on conventional IIV vaccines, which fail to protect from vaccine-mismatched viruses that have undergone significant drift in the HA head domain.

Immunization with Ad5_H1 induces stalk-specific CD4$^+$ T cells that are cross-reactive against H5 stalk

To investigate whether a single shot of Ad5_H1 could induce cross-reactive T cells to the H5 stalk, responses were characterized by flow cytometry with ICS (Figure 6), stimulating splenocytes with overlapping H5 stalk peptides (Table S2). Interestingly, unlike H1-stalk-specific T cell responses that were predominantly CD8$^+$ (Figure 3), cross-reactive H5-stalk-specific T cells were exclusively CD4$^+$ (Figures 6A–6D). Although low in magnitude, the frequencies of cross-reactive CD4$^+$ T cells were statistically significant for expression of IFN-γ (geometric mean frequency of 0.01%), IL-2 (0.02%), TNF-α (0.03%), and CD40L (0.02%), with these H5-specific CD4$^+$ T cells present at similar frequencies to H1-stalk-specific CD4$^+$ T cells. Polyfunctional analyses showed the dominant cross-reactive CD4$^+$ populations were of the same highly polyfunctional profile as H1-stalk-specific CD4$^+$ T cells (Figure 6I). Cross-reactive CD8$^+$ T cell responses against the H5 stalk were not increased over baseline (Figures 6E–6H).

Immunization with Ad5_H1 induces cross-reactive H5 stalk Abs

To facilitate the detection of cross-reactive anti-H5 Abs, we also produced H5 ectodomain (A/Vietnam/1203/2004) with a GCN4[66]

Please cite this article in press as: Bliss et al., A single-shot adenoviral vaccine provides hemagglutinin stalk-mediated protection against heterosubtypic influenza challenge in mice, Molecular Therapy (2022), https://doi.org/10.1016/j.ymthe.2022.01.011

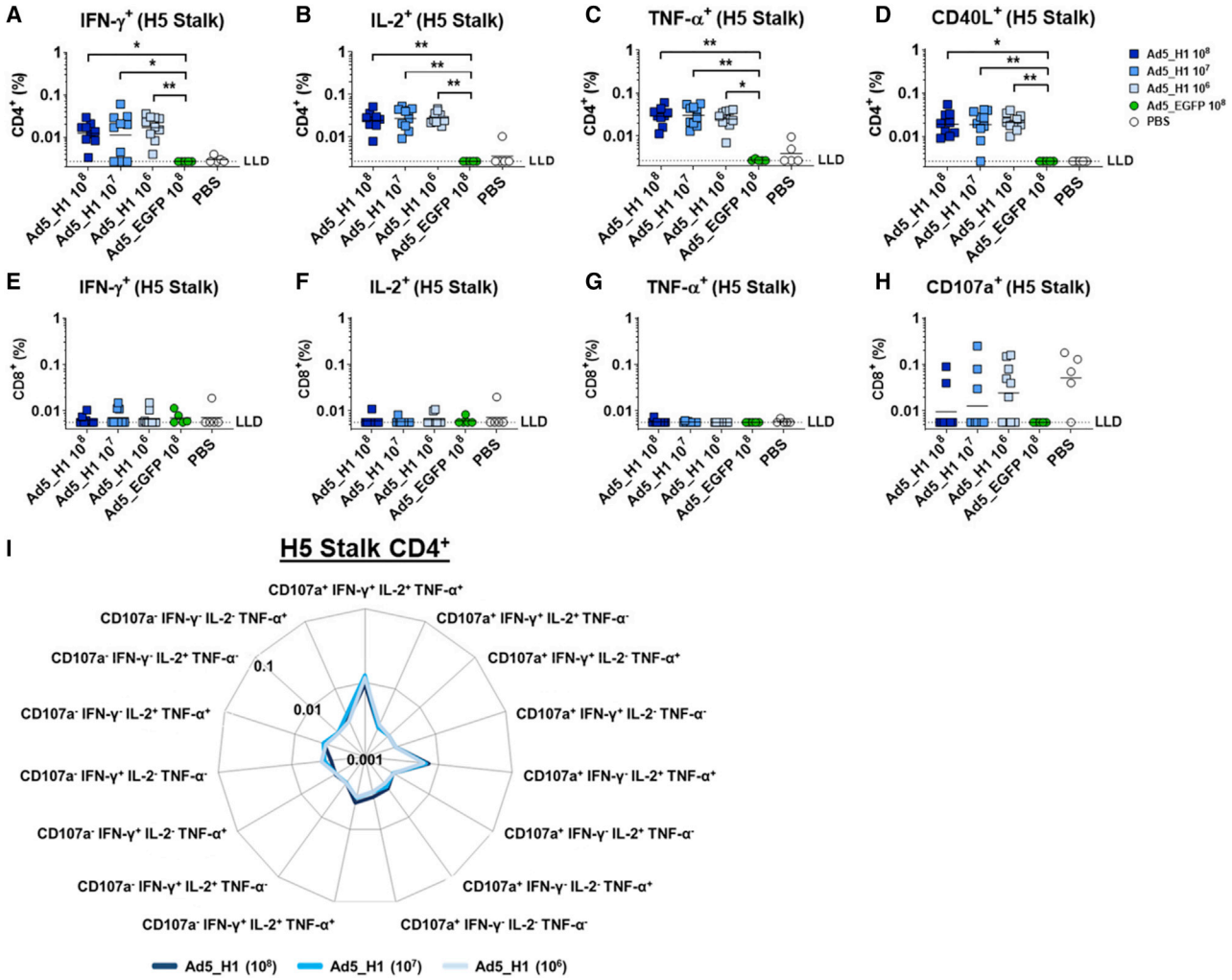

Figure 6. H5-stalk-specific T cell responses in the spleen 28 days post-vaccination

(A–H) Intracellular cytokine staining of splenocytes for (A–D) IFN-γ^+, IL-2^+, TNF-α^+, or CD40L$^+$ CD4$^+$ T cells and (E–H) IFN-γ^+, IL-2^+, TNF-α^+, or CD107a$^+$ CD8$^+$ T cells following H5 stalk peptide stimulation (see Table S2). Line indicates geometric mean, based on frequencies of cytokine-positive cells as a proportion of the parent CD4$^+$ or CD8$^+$ T cell population. Statistics were performed using the Kruskal-Wallis test with Dunn's correction for multiple comparisons against the Ad5_EGFP control; *$p < 0.05$ and **$p < 0.01$. Dashed line indicates the LLD of the assay. (I) Radar plot shows polyfunctionality of the H5-stalk-specific CD4$^+$ T cell response. Geometric mean frequencies are displayed.

trimerization domain (Figures S2C and S2D). As cross-reactive Abs are generally directed toward the HA stalk, the use of recombinant H5 would allow us to measure H5-stalk-reactive Abs. At D14 post-immunization, a dose-dependent anti-H5 IgG response was measured across the Ad5_H1 groups, with comparable responses between Ad5_H1 10^8 IFUs and the positive control H5 IIV (Figure 7A). Anti-H5 IgG responses in Ad5_H1 groups peaked at D28 (geometric mean endpoint titers 3.1×10^3 for 10^8, 2.5×10^3 for 10^7, and 6.1×10^2 for 10^6 IFUs Ad5_H1). Comparable responses were measured following Ad5_H1 10^8 and 10^7 IFUs at D28, with anti-H5 responses in both groups statistically higher than H1 IIV (Figure 7B). Low to undetectable levels of anti-H5 Ab titers were induced by H1 IIV, confirming its inability to induce cross-reactive Ab responses following a single shot. High-level anti-H5 IgG responses were elicited in mice immunized with a matched H5 IIV.

The ADCC reporter assay was also used to evaluate the potential of H5-stalk Abs in vaccinated pooled mouse sera to activate FcγRIV. MDCK cells were infected with H5N1 virus, and following addition of pooled sera and Jurkat cells expressing FcγRIV, AUC analysis of relative light units was measured to reflect the activation of Fc-effector function. A dose response was observed for Ad5_H1 at doses of 10^8–10^6 IFUs, although responses were low and there was variability between different experiments, which limits interpretation (Figure 7C). For completeness, we also performed MN assays against H5N1 but did not observe MN titers increased

Please cite this article in press as: Bliss et al., A single-shot adenoviral vaccine provides hemagglutinin stalk-mediated protection against heterosubtypic influenza challenge in mice, Molecular Therapy (2022), https://doi.org/10.1016/j.ymthe.2022.01.011

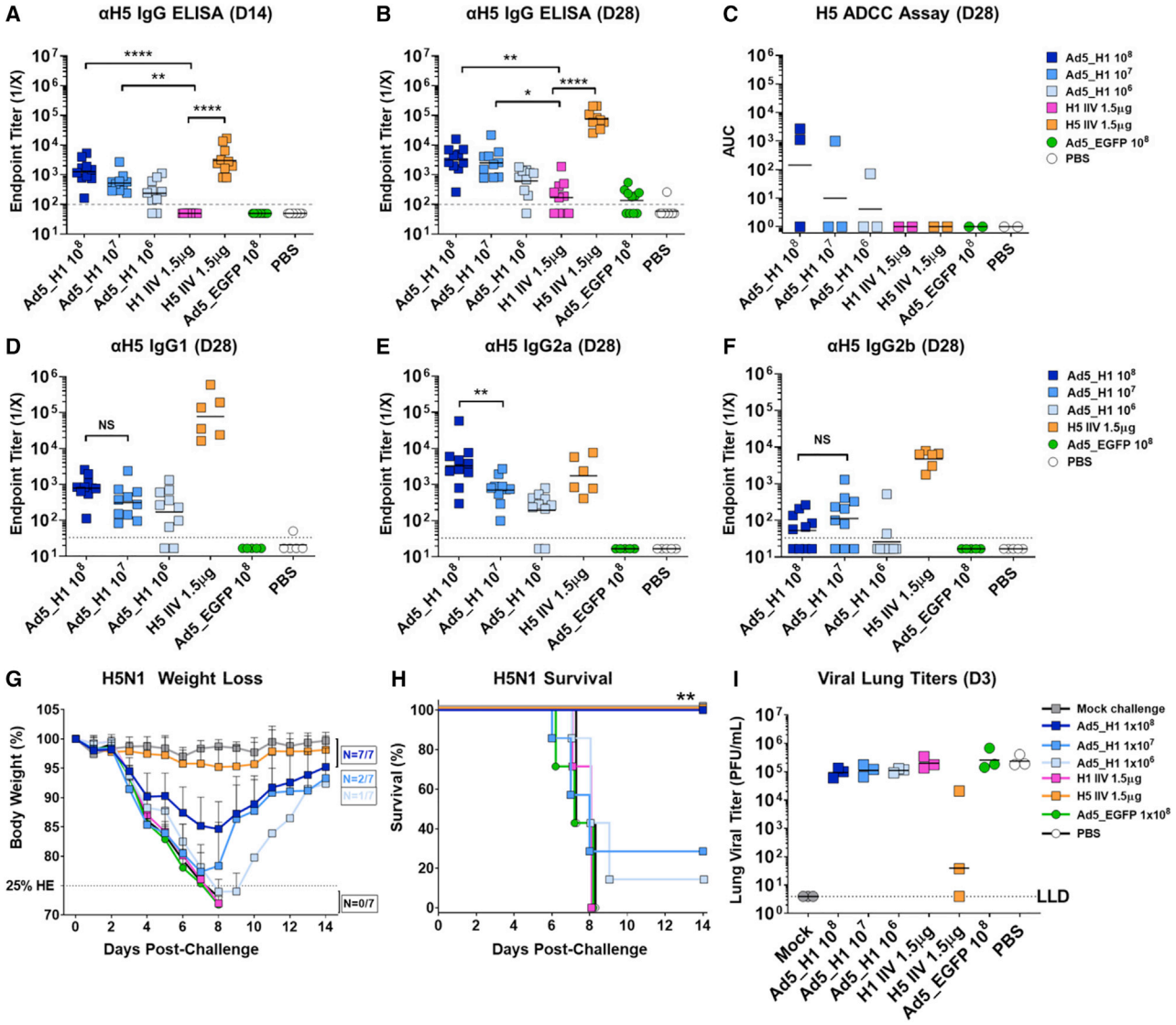

Figure 7. A single shot of high-dose Ad5_H1 (10^8 IFUs) confers 100% heterosubtypic protection from lethal challenge with H5N1

BALB/cJ female mice were immunized i.m. with a single shot of Ad5_H1 (A/California/07/2009) at doses of 10^8–10^6 IFUs, a matched monovalent split virion H1N1 IIV (BEI no. NR-20347) used at 1.5 μg, an unadjuvanted H5N1 whole virion IIV (BEI no. NR-12147) at 1.5 μg, or Ad5_EGFP, an irrelevant antigen control at 10^8 IFUs. (A–C) H5-specific humoral immune responses were measured at D14 or D28 post-immunization by (A and B) serum IgG ELISA against recombinant H5 protein (produced in-house) and (C) using a reporter-based assay to measure antibody-dependent cellular cytotoxicity (ADCC) against the H5 stalk on MDCK cells infected with H5N1 virus. For the ADCC assay, data points represent pooled sera (n = 5 mice), with each replicate derived from a separate immunization experiment. Statistical analyses were performed using the Kruskal-Wallis test with Dunn's correction for multiple comparisons against the H1N1 IIV vaccine. *$p < 0.05$, **$p < 0.01$, and ****$p < 0.0001$. (D–F) H5-specific antibody isotype subclass responses were measured against H5-GCN4. Statistical analyses were performed using the Mann-Whitney test comparing a dose of 10^8 Ad5_H1 with a dose of 10^7 IFUs. **$p < 0.01$. (G–I) At D30 post-immunization, mice were challenged i.n. with 5× mLD50 H5N1 on a PR8 background diluted in sterile PBS (50 μL). Vaccine efficacy was assessed by measuring (G) morbidity (weight loss), (H) mortality (survival), and (I) lung viral titers on D3 post-challenge (C+3). The humane endpoint was reached when mice lost 25% body weight. Weight loss data show mean and SD. For ELISA and lung viral titers, line on data points indicates the geometric mean, and the dashed gray line indicates the input serum dilution and LLD. For lung titers, this represents a minimum of one plaque counted × dilution factor. Survival significance thresholds were calculated using log rank (Mantel-Cox test), corrected for multiple comparisons comparing Ad5_H1 (10^8–10^6) and H5 IIV against H1 IIV using Bonferroni method with K = 4, with both Ad5_H1 10^8 and IIV = **$p < 0.01$.

over baseline following immunization with Ad5_H1 (Figure S3B). MN titers against H5N1 were detected following immunization with H5 IIV.

We also measured the IgG subclass of Ab induced against H5 on D28 (Figures 7D–7F). We detected a dose dependency in H5-specific Ab responses, with levels of IgG2a being higher following immunization

Please cite this article in press as: Bliss et al., A single-shot adenoviral vaccine provides hemagglutinin stalk-mediated protection against heterosubtypic influenza challenge in mice, Molecular Therapy (2022), https://doi.org/10.1016/j.ymthe.2022.01.011

with Ad5_H1 at 10^8 than with 10^7 IFUs ($p = 0.009$). Ad5_H1 elicited predominantly IgG2a > IgG1 > IgG2b Abs, mirroring findings for ELISAs against the H1 stalk (MiniHA) shown in Figures 4D–4F. Again, this IgG subclass hierarchy is also consistent with other mouse studies using Ad5-based vaccines.[46,67] H5 IIV elicited a largely IgG1 > IgG2b > IgG2a response, which was likely directed toward the immunodominant HA head domain, as supported by detectable MN activity.

Immunization with high-dose Ad5_H1 induces 100% protection from mortality against heterosubtypic H5N1 lethal influenza virus challenge in mice

Considering that we detected both cross-reactive cellular and humoral immune responses against H5 following immunization with Ad5_H1, we wanted to evaluate the capacity of this vaccine to confer heterosubtypic protection from lethal challenge as compared with conventional inactivated vaccines. Vaccine efficacy following influenza virus challenge was again assessed using three measures: (1) weight loss; (2) survival; and (3) viral lung titers. Vaccinated mice were challenged with 5× mLD_{50} of heterosubtypic H5N1 (A/Vietnam/1203/2004; 6:2 PR8 reassortant with the polybasic cleavage site in HA removed = HALo) influenza virus. In this stringent lethal challenge model, substantial weight loss was observed in all groups, except in the matched H5 IIV group, which served as a positive control in this experiment due to the high levels of H5-specific Abs induced (Figures 7A and 7B). For Ad5_H1, morbidity was dose dependent, with mean weight loss of 15.7% for the highest dose of 10^8 IFUs, 24.5% for 10^7 IFUs, and 26.8% for 10^6 IFUs Ad5_H1 (Figure 7G). By D8 following H5N1 challenge, all mice vaccinated with H1 IIV, Ad5_EGFP, or PBS reached the humane endpoint and were euthanized. Mice vaccinated with H5 IIV and Ad5_H1 at 10^8 IFUs exhibited 100% protection against mortality, which was statistically significant over groups immunized with H1 IIV and Ad5_EGFP. Mice vaccinated with 10^7 and 10^6 IFUs Ad5_H1 exhibited 29% and 14% survival, respectively (Figure 7H). Interestingly, despite clear differences in survival, viral lung titers were similar between all Ad5_H1 doses and were comparable to the viral titers detected in the lungs of mice immunized with mismatched H1 IIV, irrelevant Ad5_EGFP, or with PBS. As expected, viral titers were lower in the lungs of animals immunized with the matched H5 IIV (Figure 7I).

Again, we evaluated pathological changes in the lungs of mice euthanized between D6 and D9 post-challenge due to reaching the humane endpoint. This included mice immunized with PBS, H1 IIV, Ad5_H1 at doses of 10^7 and 10^6, and Ad5_EGFP. As before, sections were scored and imaged by a veterinary pathologist blinded to treatment groups, with the exception of the PBS vaccinated + H5N1 challenge and PBS mock challenge group. A composite score for pathology out of a total of 36 is shown in Figure S5B. Following euthanasia on D6–D9, the lungs of PBS-vaccinated (24/36) and Ad5_H1-immunized at a dose of 10^7 (26/36), Ad5_H1-immunized at a dose of 10^6 (24/36), H1-IIV-immunized (30/36), and Ad5_EGFP-immunized (24/36) mice had similar pathological scores, with the lungs of mice immunized with H1 IIV scoring most severely (Figure S5B). No mice in the Ad5_H1 10^8 group were euthanized before D14, as a result of limited weight loss. We collected the lungs of surviving animals upon termination of the experiment (D14), including lungs from PBS mock challenged mice, mice immunized with Ad5_H1 at 10^8 (n = 3) and H5 IIV (n = 3), and surviving mice from Ad5_H1 groups at doses of 10^7 (n = 2) and 10^6 (n = 1). On D14 post-challenge, pathological scores for lungs of PBS mock challenged (2/36) and the matched H5-IIV-vaccinated animals (3/36) were minimal and were considered normal. All mice in the Ad5_H1 10^8 group survived, and at D14, the pathological scores were similar for these and the few surviving mice immunized with 10^7 and 10^6 IFUs (18–21/36).

Histological sections revealed general findings that were comparable between the groups (Figure 8). Inflammation affecting the alveoli was predominantly composed of neutrophils, with some lymphocytes, plasma cells, and macrophages. Inflammation of the bronchi and bronchioles was neutrophilic with few plasma cells and macrophages. In addition, perivascular inflammation was composed of lymphocytes and plasma cells. However, it was noted that the lungs of H1-IIV-immunized mice on D7 and D8 had large regions of consolidation, where the alveolar spaces were effaced by infiltrating inflammatory cells and/or type II pneumocyte hyperplasia with loss of septal architecture (Figures 8Aii and 8Avii). Intraluminal debris was also noted (indicated by black arrowhead). Type II pneumocyte hyperplasia and intraluminal debris were also noted in the lungs of Ad-vaccinated mice (10^7 and 10^6) on D7–D9. On D14, the lungs of surviving Ad5_H1 mice immunized with 10^7 (n = 2: Figures 8Axi, 8Biii, and 8Bvii) and 10^6 IFUs (n = 1: Figure 8Axii) showed multifocal areas of consolidation, with lymphocytic inflammation, spindle cells, and, in some cases, scant collagen. Type II pneumocyte hyperplasia was also noted. In mice immunized with Ad5_H1 at 10^8 (100% survival), inflammation was considered to be predominantly lymphocytic, with ~25%–50% of the lung affected (see Figures 8Bii and 8Bvi). Localized hemorrhage was observed in the lungs of surviving mice, which has previously been described following challenge of mice with H5N1.[68] On D14, the lungs of H5-IIV-immunized mice had isolated bronchi or bronchioles with a few lymphocytes or lymphoplasmacytic aggregates, and sections were largely similar to PBS mock challenged animals (Figure 8B), consistent with sterilizing protection conferred by a matched vaccine. In conclusion, a single shot of high-dose Ad5_H1 can confer complete protection from mortality and partial protection from lung damage, even against lethal challenge with a mismatched, potentially pandemic influenza virus.

DISCUSSION

It is clear that we urgently need improvements, or alternatives, to conventional influenza virus vaccines. The strain specificity, over-reliance on egg-based manufacturing, and the need to reformulate and re-administer vaccines on an annual basis has prompted the goal of developing a "universal" influenza virus vaccine. We envisage two main applications for a universal influenza virus vaccine. The first would be an immunization regimen that stimulates broad and durable heterosubtypic protection against multiple IAVs lasting several years.[69] As a result, vaccination approaches will likely require

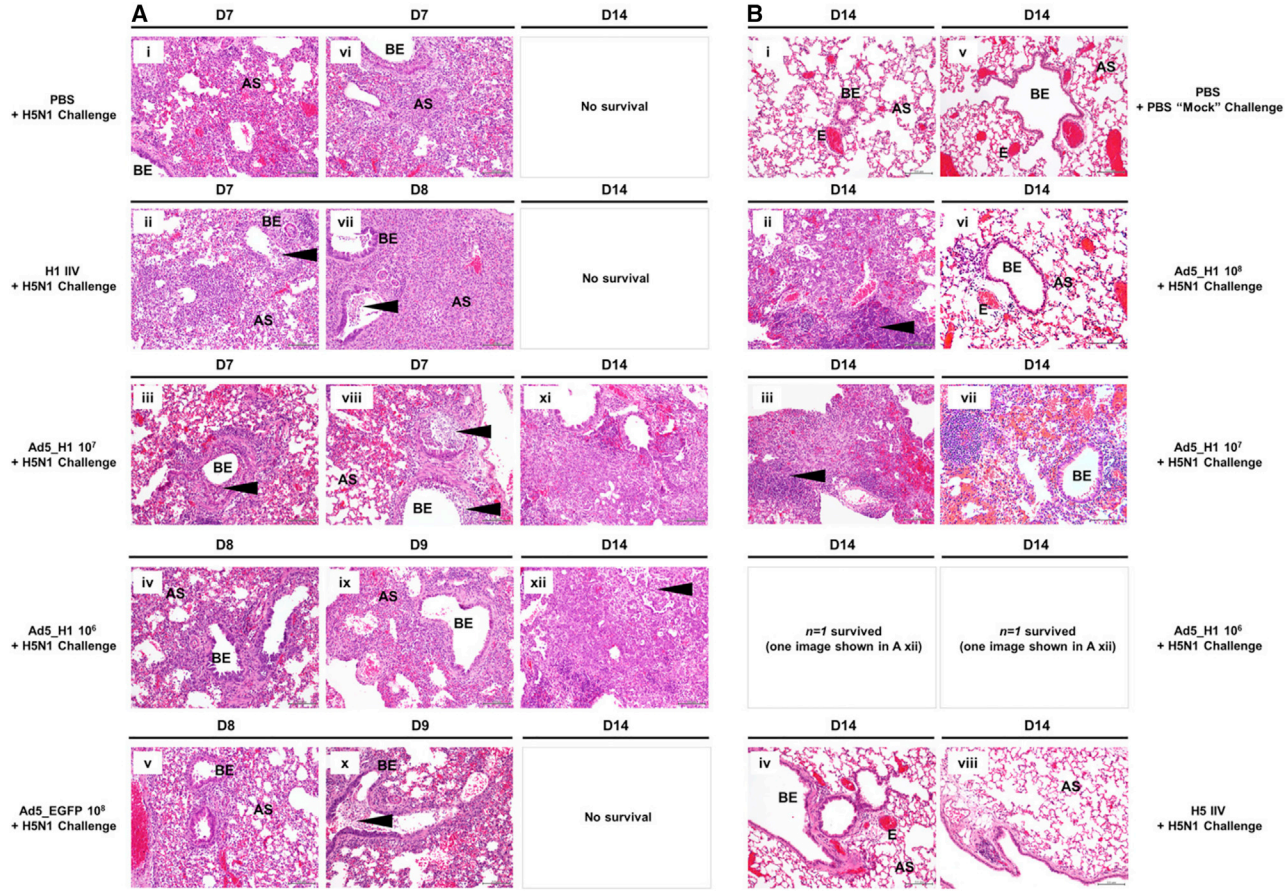

Figure 8. H&E staining of murine lung sections following challenge with H5N1 virus

BALB/cJ mice were challenged i.n. with H5N1 virus at D30 following i.m. immunization with (A) PBS, an H1 IIV at 1.5 μg, Ad5_H1 at doses of 1×10^7 and 1×10^6 IFUs, or Ad5_EGFP at 1×10^8 IFUs. (B) D14 post-challenge sections from animals immunized with Ad5_H1 at 1×10^8 IFUs (100% survival), Ad5_H1 at 1×10^7 IFUs (n = 2/7 survived), Ad5_H1 at 1×10^6 IFUs (n = 1/7 survived), and the positive control immunization group with matched H5 IIV (100% survival). Additional control groups included mock challenge with PBS. Lungs were harvested when animals reached the humane endpoint (≤25% body weight loss). For groups where survival was 100%, lungs were harvested upon termination of the experiment at D14 post-challenge (n = 3/group). Lungs were inflated with 10% formalin, fixed and processed for paraffin embedding, and 5-μm sections stained for H&E. Regions of the lung anatomy are indicated on sections. Black arrowheads indicate interesting observations, including substantial intraluminal debris (Aii, Aiii, Avii, Aviii, Ax, and Axii) or the formation of clusters of lymphocytes and plasma cells (Bii and Biii). Images represent sections from at least one animal, which were closest to the average pathological score (Figure S5B), as determined by a veterinary pathologist who was blinded to the vaccine treatment groups. Images were captured using an Olympus BX43 and an Olympus DP21 Digital Camera system under 200× magnification. Scale bars represent 100 μm.

sequential prime:boost immunization regimens with different immunogens, vaccine formulations, and/or adjuvants to achieve the right phenotype, magnitude, and breadth of protection.[3] Another approach that should be considered is a single-shot vaccine capable of eliciting rapid, cross-reactive responses directed toward conserved epitopes. Such a vaccine should protect against drifted seasonal strains, as well as emerging viruses that present a pandemic threat. Vaccines with this target product profile should be compatible with rapid scale-up manufacturing, and the product should be well suited to stockpiling without specialized cold-chain requirements. Non-replicating Ad vectors are one promising platform in this regard. They elicit robust cellular and humoral immune responses in multiple species,[46,50,70,71] including humans.[72–79] Importantly, they can be lyophilized with minimal losses to immunogenicity[80–83] and are thermostable at 4°C and −20°C for prolonged periods of time, making them well suited for pandemic preparedness and stockpiling[84] and the logistics of global distribution.

In this study, we constructed a non-replicating Ad-vectored vaccine expressing a secreted form of influenza virus H1. In a series of single-shot immunogenicity and *in vivo* challenge studies in mice, we compared the efficacy of this vaccine head to head with conventional IIVs. We determined that a single shot of Ad5_H1 can rapidly induce Abs with diverse functional activities. More importantly, Ad5_H1 elicited broadly protective Abs directed toward the highly conserved HA stalk. The latter finding is of considerable interest, as it is widely considered that the HA stalk is poorly immunogenic,[2,5,6] and multiple immunizations, often combined with display of the stalk on nanoparticles,[19,20]

Please cite this article in press as: Bliss et al., A single-shot adenoviral vaccine provides hemagglutinin stalk-mediated protection against heterosubtypic influenza challenge in mice, Molecular Therapy (2022), https://doi.org/10.1016/j.ymthe.2022.01.011

conjugated to carriers,[6] or formulated with adjuvants, are required to elicit protective titers of stalk-specific Abs in naive animals.[85–88] Therefore, these findings represent an advance on both IIVs and alternative universal influenza vaccines in pre-clinical development.

In a homologous H1N1 challenge experiment, HI^+-H1-specific Abs elicited by immunization with Ad5_H1 conferred 100% protection from lethal challenge in a manner comparable to a matched IIV. For vaccine regimens that produced HI^+ Abs with titers $\geq$1:40, protection from morbidity and mortality was accompanied by complete sterilizing protection in the lung. However, unlike IIV, a single shot of Ad5_H1 also rapidly induced stalk-specific Abs by D14. Swift induction of Abs has been measured in humans vaccinated with Ad vaccines against infectious diseases, including severe acute respiratory syndrome coronavirus 2 (SARS-CoV-2),[77,89,90] and this would be a desirable attribute for a pandemic vaccine. Importantly, the mechanism of protection for broadly reactive, stalk-focused Abs is completely distinct from classical, HI^+ head-specific NAbs. Stalk Abs capable of activating Fc-mediated effector mechanisms, such as ADCC or antibody-dependent cellular phagocytosis (ADCP) *in vitro*, can confer *in vivo* protection against IAV in animals.[54–56,91–93] Immunization with Ad5_H1, but not IIV, induced H1-stalk-reactive Abs that activated murine FcγRIV in an ADCC reporter assay.

In addition, a single shot of Ad5_H1 also elicited both $CD4^+$ and $CD8^+$ H1-stalk-specific T cell responses at all doses tested, whereas IIVs did not. With increasing interest in the HA stalk as a universal vaccine target, efforts have been made to identify T cell epitopes in the HA stalk,[94,95] but their specific contribution to vaccine efficacy remains largely undefined to date. The limited induction of cellular immunity by IIVs has been documented.[40–44] In addition to providing help to B cells, $CD4^+$ T cells assist in the development of $CD8^+$ responses,[96] produce cytokines, and can have direct cytolytic activity.[97,98] Considering that in human influenza virus vaccine responses, antibody responses to HA are correlated with HA-specific $CD4^+$ T cells,[99] HA-stalk-specific $CD4^+$ T cells may play a role in increasing Ab responses to the immunosubdominant HA stalk. Therefore, while the $CD4^+$ T cell responses we detected in this study are of low frequency, they could be an important component of the overall adaptive and protective immune response, especially given their cross-reactivity between H1 and H5. There is a paucity of information in the literature regarding HA-stalk-specific T cell responses in humans and mice. It is also important to note that T cell epitopes differ between species, making it difficult to predict the translational relevance of T cells that target specific CD4 or CD8 epitopes. However, a recent study identified $CD4^+$ T cell epitope "hotspots" in influenza HA that are similar between wild-type mice and transgenic mice expressing human leukocyte antigen (HLA) class II,[95] suggesting that this pre-clinical model might prove useful for evaluating T cell responses for HA-stalk-focused universal vaccines. Furthermore, clinical studies have reported responses to HA stalk T cell epitopes following immunization with universal vaccine candidates.[100] As clinical trials in humans testing HA-stalk-based vaccines advance in the near future, more detailed information regarding immunodominant HA stalk epitopes will become available, enabling more authentic parallels to be drawn between clinical and pre-clinical studies.

A vaccine capable of eliciting broad, anti-stalk Abs could provide a cross-reactive barrier of defense in the absence of well-matched anti-head Abs. In support of this, we determined that the induction of stalk-reactive Abs with Fc-mediated effector activity, combined with high frequencies of T cells specific to the H1 stalk, were sufficient to provide robust protection against cH6/1N5 lethal challenge. Both $CD4^+$ and $CD8^+$ T cells have been implicated in contributing synergistically to protection.[101,102] A broad phenotype of immunogenicity elicited by a single vaccine could represent a means to overcome antigenic drift, a factor that necessitates costly annual reformulation of seasonal IIVs. Despite complete protection from morbidity and mortality at all doses of Ad5_H1 in the cH6/1N5 stalk challenge model, some virus was detected in the lungs of these animals. This is consistent with our mechanistic understanding of how stalk-mediated Abs contribute to protection *in vivo*. In this scenario, lung cells infected with cH6/1N5 that express cH6/1 HA on the cell surface during replication would allow stalk Abs to bind the HA stalk via their Fab domain and simultaneously engage FcγRs via their exposed Fc domain,[53] thus triggering Fc-mediated effector functions. A role for alveolar macrophages in cooperating with broadly reactive Abs (neutralizing and non-neutralizing) to mediate protection *in vivo* has previously been described.[56] Therefore, it is likely that multiple immune components work in concert to limit viral pathogenesis.

Beyond protection from matched (pH1N1) and mismatched challenge viruses (cH6/1N5), we also confirmed cross-reactivity against an antigenically distinct avian influenza H5 subtype. Interestingly, prior to H5N1 influenza virus challenge, Ad5_H1 vaccination with doses of 10^8 and 10^7 IFUs induced comparable non-neutralizing anti-H5 IgG responses. Furthermore, cross-reactive H5-stalk-specific $CD4^+$ T cell responses, although low frequency, were also comparable, with no distinct difference in the frequency, profile, or polyfunctionality of T cells induced. However, the difference in protection against H5N1 lethal challenge virus was striking, with 100% survival in the Ad5_H1 10^8 IFUs group but only 29% in the Ad5_H1 10^7 IFUs group. The most notable difference in the immune response between 10^8 and 10^7 IFUs of Ad5_H1 was in H5-specific IgG2a titers. The Th1 phenotype of the $CD4^+$ T cells induced may help drive the IgG2a response. However, while this subclass dominated both the H1-stalk-specific and H5-stalk-specific responses, the magnitude of H5-stalk-specific IgG2a Abs were a log lower than H1-stalk IgG2a, particularly when comparing equivalent vaccine doses. These differences were also reflected in the induction of ADCC by H1-stalk-reactive Abs versus H5-stalk-reactive Abs, the latter of which was substantially lower. This suggests that, in the absence of HI^+ Abs, a minimal threshold of effector function activity via FcγRIV might be required for efficient stalk-mediated protection *in vivo*. Equally, we cannot exclude the possibility that the triggering of other activating Fcγ receptors expression on various murine cell types could further contribute to protection *in vivo*. Despite detecting significant, albeit low, frequencies of $CD4^+$ T cells that were cross-reactive with the H5 stalk, we did not detect

any cross-reactive $CD8^+$ T cells following immunization with Ad5_H1. This was unexpected, as Ad vectors are well established for their robust induction of $CD8^+$ responses. The stalks of H1 and H5 share ~76% amino acid sequence identity. However, it is possible that common $CD8^+$ T cell epitopes do not exist between the H1 and H5 stalks, or responses are not induced by a single immunization in naive animals. This finding warrants further investigation but could potentially be overcome in the future by including adjuvants or by performing prime:boost immunization regimens. Unlike the cH6/1N5 challenge, no reduction in viral lung titers was observed in the H5N1 challenge model in animals immunized with Ad5_H1. Again, it is likely that multiple components of the immune response may cooperate to confer protection from disease.[101] The limited clearance of virus from the lung in this model may have been affected by the lack of $CD8^+$ T cells and, potentially, sub-optimal ADCC activity of H5 cross-reactive stalk Abs. The inclusion of nucleoprotein (NP), which is a known target for $CD8^+$ T cells and has been associated with limiting symptomatic disease in humans[103] and providing broad protection in animals,[104,105] could be included in Ad-based vaccines and may increase viral clearance and maximize the efficacy of universal influenza virus vaccines.

Overall, several factors likely contribute to the increased breadth of protection from lethal challenge observed for Ad5_H1, as compared with IIV. Ad vaccines are known to stimulate multiple innate immune signaling pathways upon entry and intracellular trafficking, which shape the magnitude and phenotype of the ensuing immune response.[106–108] In contrast, unadjuvanted IIV is limited in its ability to stimulate pathogen-recognition receptors.[109] Ad vectors also elicit robust cellular immunity,[46,106,110] whereas immunization with IIV is not associated with the induction of significant cellular immune responses. In addition, it is well established that Ad vectors can facilitate antigen persistence,[45,110] which may result in an ongoing source of antigen for antigen-presenting cells (APCs) and/or germinal centers. This persistence is in contrast with IIV immunization, in which antigen availability is limited to the initial bolus injection. In support of this, a recent study has demonstrated that a slow-release delivery approach for an HIV-1 Env antigen, rather than bolus immunization, resulted in a qualitatively superior immune response with increased B cell diversity and target antigen binding specificities.[111] Increased understanding of the precise mechanisms that confer the broad protection from lethal challenge observed in this study will be important in contributing to the identification of correlates of protection for stalk-focused universal influenza vaccines.

The use of a secreted form of HA may have helped to expose broadly cross-protective stalk epitopes. Future studies comparing this with full-length HA will shed further light on mechanisms underlying the increased immunogenicity of the immunosubdominant HA stalk in this study. With regard to the use of secreted protein containing a fibritin foldon trimerization domain, this domain has previously been reported to be immunogenic following three repeat immunizations in animal models.[112] In this manuscript, we administered a single immunization with an H1 antigen containing fibritin. Nonetheless, to negate any issues when performing serological assays, we used ELISA coating antigen with an alternate trimerization domain. A viral glycoprotein antigen containing the fibritin trimerization domain, prefusion (F) glycoprotein from respiratory syncytial virus (RSV), has already been tested in a phase I clinical trial in humans in a homologous prime:boost regimen (NCT03049488).[113] Sequential immunization resulted in boosting of F-specific NAbs. If the use of secreted HA does indeed enhance accessibility of immunosubdominant HA stalk epitopes, it may be possible to use structure-guided immunogen design to develop stable, trimeric HAs that lack any trimerization domain for future clinical use. This has been achieved for RSV prefusion F, for which cysteine-constrained trimers have successfully been designed.[114]

Although currently undergoing clinical evaluation as a vaccine for SARS-CoV-2, Ad5 may not be the ideal vector for clinical use in humans, due to high seroprevalence that could negatively impact immune responses to the vaccine antigen. In this study, we used Ad5 as a tool to clearly demonstrate proof of concept for our hypothesis: that it is possible to elicit protective levels of immunity directed toward the immunosubdominant influenza virus HA stalk with a single-shot vaccine. These data suggest that, with the right immunogen, in combination with the optimal Ad vaccine platform, it may be possible to develop a broadly protective, single-shot vaccine targeting the HA stalk domain for pandemic preparedness. The diversity of Ad vectors with minimal pre-existing immunity in humans that are available, and their compatibility with several innovative stalk-based immunogens currently undergoing pre-clinical evaluation (i.e., headless HAs and chimeric HAs), highlight the feasibility of advancing similar approaches for future clinical development.

MATERIALS AND METHODS

Cell lines and culture media

Expi293F cells (Life Technologies, Carlsbad, CA) were maintained in suspension in serum-free Expi293F medium (Gibco, Gaithersburg, MD) according to manufacturer's instructions and incubated at 37°C in a humidified atmosphere of 8% CO_2 on a shaking platform. T-REx-293 cells (Life Technologies, Carlsbad, CA) were cultured in high-glucose Dulbecco's modified Eagle's medium (DMEM) (Sigma-Aldrich, St. Louis, MO) supplemented with 10% fetal bovine serum (FBS) (Gibco, Gaithersburg, MD), 4 mM L-glutamine (Sigma-Aldrich, St. Louis, MO), 100 μg/mL penicillin-streptomycin (Sigma-Aldrich, St. Louis, MO), and 5 μg/mL blasticidin S (Gibco, Gaithersburg, MD) and incubated at 37°C in a humidified atmosphere of 5% CO_2 in air. Cell lines were purchased directly from the vendor and have associated lot numbers. Murine splenocytes and blood lymphocytes were cultured in media denoted "R10" for flow cytometry assays, consisting of Roswell Park Memorial Institute (RPMI) media supplemented with 10% FBS, 100 μg/mL penicillin-streptomycin, and 2 mM L-glutamine. MDCK and MDCK cH6/1 cells were cultured in 1× minimum essential medium (MEM) supplemented with 100 μg/mL streptomycin, 2 mM L-glutamine, 0.15% Na_2HCO_3, 50 mM 4-(2-hydroxyethyl)-1-piperazineethanesulfonic

acid (HEPES), and 10% FBS. FBS was substituted with 0.4% BSA for plaque assay. The MDCK cell line stably expressing the cH6/1 has previously been described.[63] All cell lines used in this study were routinely tested using PlasmoTest (InvivoGen, San Diego, CA) and were determined to be mycoplasma negative prior to use.

Recombinant protein and antibody expression, purification, and validation

We engineered and expressed recombinant headless HA (i.e., MiniHA #4900 based on H1 A/Brisbane/59/2007)[23] and H5 (A/Vietnam/1203/2004) proteins with the GCN4 isoleucine zipper trimerization domain[66] from *Saccharomyces cerevisiae* and a C-terminal 6×-histidine (6XHIS) tag. Sequences were codon optimized for *Homo sapiens*, synthesized by GenScript (Piscataway, NJ) and provided in expression plasmid pcDNA3.1(+) for transfection into Expi293F cells using 4 μg/mL polyethylenimine (PEI). Expi293F cells were grown in serum-free Expi media according to manufacturer's instructions. Soluble secreted trimeric HA protein was purified from the cell-free supernatant (SN) 96 h post-transfection using nickel-nitrilotriacetic acid (NiNTA) affinity chromatography (QIAGEN, Hilden, Germany). Protein concentration was assessed by NanoDrop ND-1000 under settings for Protein 280. Purified MiniHA was validated for size and multimerization by anti-HIS western blot (w.blot) comparing 50 ng denatured (95°C for 5 min; +dithiothreitol [DTT]) and non-denatured (unboiled; no DTT) on a 10% Mini-Protean TGX Pre-cast gel (Bio-Rad, Hercules, CA). Recombinant proteins were further checked for structural integrity by performing ELISAs using a panel of previously described mAbs that recognize conformational epitopes on the HA stalk. These antibodies include human mAbs CR9114[34] and FI6,[35] as well as mouse mAbs KB2[27] and GG3.[36] ELISA plates were coated with 2 μg/mL recombinant HA protein in 50 μL carbonate buffer. Human mAbs CR9114 and FI6 were used at a starting concentration of 1 μg/mL, followed by a 10-fold serial dilution, whereas murine mAbs KB2 and GG3 were used at 3.33 μg/mL, followed by a 3-fold serial dilution. Negative controls included species-specific IgG subclass-matched isotype controls and secondary-only antibody controls run on each plate. Validation by w.blot and ELISA is summarized in Figure S2. Full-length H1 (A/California/07/2009) protein used for mouse serum IgG ELISAs in Figures 2A and 2B was obtained from BEI Resources (NR-44074; lot no. 63,979,139). Plasmids encoding the heavy and light chain for previously described broadly cross-reactive anti-HA stalk antibodies, CR9114 and FI6, were provided by Dr. Patrick Wilson and Dr. Carole Henry (University of Chicago). Antibodies were expressed in 293A cells adapted to low IgG FBS and purified using protein A beads (Thermo Fisher Scientific, USA), as described previously.[115]

Adenoviral vaccine engineering and production

DNA corresponding to influenza HA from H1 A/California/07/2009 in soluble secreted form was synthesized by BioBasic (ON, Canada). The H1 immunogen was codon optimized for *Homo sapiens*[116] and engineered for secretion by removal of the transmembrane (ΔTM) domain sequence of HA (Figure 1A), which was replaced with a heterologous carboxy (C)-terminal trimerization domain (i.e., fibritin foldon).[32,33] A 6XHIS tag was also engineered at the C terminus to facilitate confirmation of H1 expression by anti-HIS w.blot (Figure 1B). The correct assembly of secreted H1 was confirmed by ELISA using mAbs that bind to conformational epitopes on the HA stalk domain (Figures 1C and 1D). Once validated, the final H1 antigen sequence was sub-cloned into *Not*I digested plasmid pENTR, upstream of a CMV promoter for subsequent homologous recombination into a non-replicating Ad5 bacterial artificial chromosome (BAC) backbone using Gateway technology (Life Technologies, Carlsbad, CA), as previously described.[46,117] A control Ad5 vaccine expressing irrelevant antigen, EGFP, was engineered in a similar manner. Ad5 genomes were linearized by *Pac*I to release the infectious viral genome and transfected into T-REx-293 cells (Life Technologies, Carlsbad, CA). The Ad5_H1 or control Ad5_EGFP vaccines were amplified, purified by two rounds of cesium chloride banding, and titrated at the Jenner Institute Viral Vector Core Facility (University of Oxford, UK).

Vaccines

A number of IIV constructs were included in challenge experiments as a comparator for the phenotype of immunity conferred by traditional influenza vaccine platforms. These included a monovalent split-virion vaccine based on H1 A/California/07/2009 to act as an antigen-matched control to the H1 encoded in our Ad5 vaccine and as a positive control for sterilizing protection in a homologous pH1N1 challenge model. This reagent was obtained through BEI Resources, National Institute of Allergy and Infectious Diseases (NIAID), NIH: Influenza A (H1N1) 2009 Monovalent Vaccine, NR-20347 (lot no. UF867AD), and was used at a dose of 1.5 μg HA, administered i.m. To act as a positive control for sterilizing protection in H5N1 challenge experiments, a non-adjuvanted, inactivated whole virion A/H5N1 (A/Vietnam/1203/2004) influenza vaccine was obtained through BEI Resources, NIAID, NIH: NR-12147 (lot no. VNVIF008A) and was also used at 1.5 μg HA, administered i.m.

Influenza challenge viruses

A wild-type A/Netherlands/602/2009 (pH1N1) virus was used as a homologous H1 challenge virus. This virus has two amino acid non-synonymous substitutions in the HA head domain when compared with the H1 encoded in the Ad5_H1 construct (P91S; I323V; H3 numbering).[118] A chimeric H6/1 virus was used in the stalk-matched challenge. This virus expresses a chimeric HA, consisting of an H6 HA head domain (A/mallard/Sweden/81/2002) and an H1 stalk domain (A/California/04/2009), matched to the H1 stalk in our Ad5-H1 vaccine. The cH6/1N5 virus is a 6:2 reassortant virus on an A/Puerto Rico/8/1934 backbone, with an A/mallard/Sweden/86/2003 N5 neuraminidase (NA). The heterosubtypic H5N1 challenge virus was a 6:2 re-assortment virus of low pathogenicity avian A/Vietnam/1203/2004, in which the polybasic cleavage site was removed (HALo), and N1 from A/Vietnam/1203/2004 in an A/Puerto Rico/8/1934 backbone.

Generation of viral challenge stock

One hundred PFUs of influenza virus was injected into 10-day-old embryonated chicken eggs and incubated at 37°C for 2 days. Eggs

Please cite this article in press as: Bliss et al., A single-shot adenoviral vaccine provides hemagglutinin stalk-mediated protection against heterosubtypic influenza challenge in mice, Molecular Therapy (2022), https://doi.org/10.1016/j.ymthe.2022.01.011

were then moved to 4°C and allowed to rest overnight. The allantoic fluid was harvested and cleared through centrifugation at 3,000*g* for 10 min at 4°C in an Eppendorf 5810R using an A-4-81 rotor. Cleared supernatant was tested via hemagglutination assay and frozen into single-use aliquots at −80°C.

Determination of viral titer

MDCK cells were plated in 6-well dishes at a concentration of 8×10^5 cells/well and allowed to incubate overnight at 37°C with 5% CO_2. Virus in allantoic fluid was diluted in log steps to a final dilution of 10^{-8}, and 250 μL of each dilution was added to a monolayer of MDCK cells after washing with PBS. Adsorption was allowed to proceed for 1 h with intermittent shaking every 10–15 min. PBS was then added to wash off non-adsorbed virus, and an agar overlay consisting of 0.01% diethylaminoethyl (DEAE)-dextran, 0.64% agar, and 1 μg/mL of L-(tosylamido-2-phenyl) ethyl chloromethyl ketone (TPCK)-treated trypsin in 1× MEM was added and allowed to solidify at room temperature. Infection was allowed to proceed for 48 h at 37°C and 5% CO_2 or until visible plaques appeared. Plaques were counted following crystal violet staining, and titer was determined as a function of the number of plaques per well, the dilution factor, and volume added per well.

Mice

All animal studies were approved by the Icahn School of Medicine at Mount Sinai Institutional Animal Care and Use Committee (IACUC-2017-0170) and were carried out at The Center for Comparative Medicine and Surgery (CCMS) vivarium. All mice were female BALB/cJ mice (Jackson Laboratory, Bar Harbor, ME) aged 7 to 8 weeks at time of vaccination (n = 5–10 mice/group).

Mouse immunogenicity and challenge study design

Mice arriving at the vivarium were given an acclimatization period of ~6 days before the commencement of procedures. Mice were randomly assigned to individually ventilated cages (n = 5), with each cage acting as an experimental unit forming part or all of a single vaccination group. Mice were bled via the submandibular route at day −2 (D−2) and then vaccinated at D0 i.m. with vaccine diluted in 50 μL sterile PBS (Figure 1E). Test vaccination groups consisted of 10^8, 10^7, or 10^6 IFUs of Ad5_H1 vaccine. Control groups included 10^8 IFUs Ad5_EGFP vaccine, 1.5 μg H1 IIV, 1.5 μg H5 IIV, or sterile PBS alone (50 μL final volume). Mice were bled via the submandibular route at D14 and/or D28. Subsets of mice were humanely euthanized by increasing concentration of CO_2 for splenocyte analyses at D28, and remaining mice were subsequently challenged intranasally (i.n.) with influenza virus at 5×–10× mouse LD_{50}. Influenza-virus-challenged mice were monitored for 14 days for weight loss and were humanely euthanized by increasing concentration of CO_2 if their weight dropped below 75% of their individual pre-challenge weight. Surviving mice were humanely euthanized 14 days post-challenge.

Determination of mouse LD_{50}

Influenza virus was diluted to 10^5 PFUs/50 μL and further diluted in log steps to reach 10 PFUs/50 μL. Mice were anesthetized using a ketamine/xylazine mixture and infected i.n. with 50 μL of a particular dilution. Weight loss was monitored for 14 days, and mice dropping below 75% initial body weight were humanely sacrificed. The mouse LD_{50} was calculated based on the survival data by determining the titer at which 50% of the mice would survive.[119]

Influenza virus challenge weight loss and survival

Post-challenge weights were normalized to the defined pre-challenge weight for each mouse. Mice were humanely euthanized if 25% weight loss against pre-challenge weight was measured. Survival curves denote the day post-challenge each mouse was humanely euthanized. Survival significance thresholds were calculated using a log rank (Mantel-Cox) test with manual Bonferroni correction for multiple comparisons.

Blood and organ harvesting

For serum blood sampling, blood was drawn via submandibular puncture and collected in Microvette CB300 capillary blood collection tubes with clot activator (Sarstedt) and were then centrifuged at 15,000*g* for 5 min, serum aliquoted, and stored at −20°C. Maximal blood sampling throughout the duration of the studies did not exceed recommended guidelines per total blood volume (TBV) for mice, as established by the National Center for the Replacement, Refinement and Reduction of Animals in Research (NC3Rs): a maximum <10% TBV on any single occasion and <15% TBV within a 28-day period. For spleen harvesting, mice were administered xylazine/ketamine intraperitoneally (i.p.) and terminally exsanguinated via cardiac puncture into Microtainer with clot activator (BD Biosciences), followed by cervical dislocation and spleen dissection.

Organ processing

Spleens were mechanically disrupted through a 40-μm cell strainer into PBS and then pelleted by centrifugation at 450*g* for 5 min. SNs were discarded and splenocytes resuspended in ammonium-chloride-potassium (ACK) (0.15M NH_4Cl, 10 mM $KHCO_3$, and 100 mM EDTA-Na_2 in water) lysing buffer and incubated for 5 min at room temperature, vortexing at the start and end of incubation. PBS was added per sample to stop the lysis, samples were pelleted by centrifugation at 500*g* for 5 min, and then SN was discarded. Samples were resuspended in R10, and cell debris clump was removed and then re-pelleted by centrifugation 500*g* for 5 min. Splenocytes were resuspended in R10 for counting and then re-suspended to 25×10^6 splenocytes/mL.

Peptides for T cell assays

The following reagent was obtained through BEI Resources, NIAID, NIH: Peptide Array, Influenza Virus A/California/07/2009 (H1N1) pdm09 Hemagglutinin Protein, NR-19244. NR-19244 is a 139-peptide array spanning the influenza HA from A/California/07/2009 (pH1N1), using 15-amino-acid-long peptides with an 11-amino-acid overlap. A peptide pool for the H1 stalk domain only (65 peptides) was reconstituted according to Table S1. The following reagent was obtained through BEI Resources, NIAID, NIH: Peptide Array, Influenza Virus A/Vietnam/1203/2004 (H5N1) Hemagglutinin Protein, NR-18974. NR-18974 is a 93-peptide array spanning the

influenza virus HA from A/Vietnam/1203/2004 (H5N1), using 17-amino-acid-long peptides with an 11-amino-acid overlap. A peptide pool for the H5 stalk domain only (45 peptides) was reconstituted according to Table S2. Lyophilized peptides were reconstituted in DMSO at 20 or 30 mg/mL and then peptides were pooled in 200 μg/mL working stocks for use in flow cytometry assays.

Cell stimulation and staining for intracellular cytokine staining assay

Splenocytes or PBMCs were stimulated in R10 medium containing anti-mouse CD28 (1:1,000; BD Biosciences), brefeldin A (1:1,000; BD Biosciences), monensin (1:1,000; BD Biosciences), and anti-mouse CD107a-PE (1:200; BioLegend) for 6 h at 37°C in 5% CO_2. Stimulations consisted of either 1 μg/mL of pooled H1- or H5-stalk peptides (Tables S1 and S2) or an equivalent volume of DMSO as a negative control. Separate splenocytes and selected PBMC samples (when sample volume permitted) underwent stimulation with a combination of 0.5 μg/mL phorbol 12-myristate 13-acetate (PMA) (Sigma-Aldrich, St. Louis, MO) and 1 μg/mL ionomycin (Sigma-Aldrich, St. Louis, MO) as a positive control. After stimulation, plates were stored at 4°C overnight protected from light. Cells were then pelleted by centrifugation at 500*g* for 5 min in an Eppendorf 5810R centrifuge, and samples were incubated with Fc block (1:100; BD Biosciences) for 10 min at 4°C. Cells were washed in fluorescence-activated cell sorting (FACS) buffer and incubated with surface-staining cocktail for 30 min at 4°C protected from light (see Table S3). After incubation, cells were washed in FACS buffer and then incubated in Fixation/Permeabilization buffer (BD Biosciences) for 10 min at 4°C. Cells were washed in 1× Permeabilization buffer (BD Biosciences) and then incubated with the intracellular staining cocktail for 30 min at 4°C protected from light (see Table S3). Samples were washed twice in 1× Permeabilization buffer and once in FACS buffer and then resuspended in FACS buffer. Samples were acquired on an LSRII cytometer (BD Biosciences) using FACSDiva v.7.03 (BD Biosciences), with the relevant single fluorochrome compensation controls (UltraComp eBeads; Thermo Fisher Scientific, Waltham, MA) and photon multiplier tube voltages set by daily acquisition of Cytometer Setup and Tracking beads (BD Biosciences).

ELISA—total IgG

Immulon 4HBX flat bottom 96-well plates (Thermo Fisher Scientific, Waltham, MA) were coated overnight at 4°C with recombinant MiniHA, H1 or H5 protein at 2 μg/mL diluted in 50 μL of 50 mM carbonate Na_2CO_3 buffer (Sigma-Aldrich, St. Louis, MO). The following day, plates were washed using 1× PBS (Life Technologies, Carlsbad, CA) containing 0.1% Tween 20 (Millipore, Burlington, MA) and blocked with 200 μL blocking buffer: PBS containing 1% (w/v) BSA (Sigma-Aldrich, St. Louis, MO) for at least 1 h at room temperature. After washing with PBS Tween, a 1:100 dilution of mouse sera was added to the plate in duplicate and a 3-fold serial dilution in blocking buffer performed, resulting in a final volume of 100 μL/well. Plates were incubated for 2 h at room temperature on an orbital shaker. A positive control mAb, KB2 (mouse IgG2a), which binds to the HA-stalk of H1 and H5 HAs, was used on each plate at a final concentration of 10 μg/mL. A matched isotype control (clone no. MOPC-173 mouse IgG2a; Abcam, Cambridge, UK) was used as a negative control on every plate. Additional controls on each plate included naive, unvaccinated mouse sera and secondary antibody-only controls. After washing, 100 μL goat anti-mouse IgG horseradish peroxidase (HRP)-conjugated secondary Ab (1:5,000; Millipore, Burlington, MA) was added to the plate. After a 1-h incubation at 37°C, the plate was washed and developed using 100 μL SigmaFast o-phenylenediamine dihydrochloride (OPD) (Sigma-Aldrich, St. Louis, MO) tablets diluted in water. Development was stopped with 50 μL 3M HCl after a set period of time: 10 min for MiniHA and H5 ELISA and 6 min for H1 ELISA. Plates were read for optical density (OD) at 492 nm.

ELISA—IgG subclass

ELISAs were performed as above with modifications: serial dilutions of vaccinated mouse sera started at 1:33.3 instead of 1:100. Naive unvaccinated controls were also added at this final dilution. Following the 2-h incubation, 50 μL of biotin-conjugated secondary rat antibodies specific for each isotype, anti-mouse IgG1 (BD Biosciences, Franklin Lakes, NJ), anti-mouse IgG2a (BD Biosciences, Franklin Lakes, NJ), and anti-mouse IgG2b (BD Biosciences, Franklin Lakes, NJ), were diluted to 1 μg/mL in blocking buffer and added to the plate. After a 1-h incubation shaking at room temperature, 50 μL of ExtrAvidin-Peroxidase (1:2,500; Sigma-Aldrich, St. Louis, MO) was added directly to each well, without washing, and the plate was incubated for 30 min shaking at room temperature. Plates were washed prior to development using SigmaFast OPD solution for 10 min, as described above.

Analysis of ELISA data

The ELISA baseline was defined as the mean plus three standard deviations (3SDs) of the lowest dilution of naive sera OD values across all plates in a single run (i.e., 1:100 of naive sera for standard IgG ELISAs or 1:33.3 for isotype ELISAs). The mean of test sera duplicate values was calculated for each dilution. Endpoint titers were calculated using GraphPad Prism v.8.2.1 and represent the X-intercept with the defined baseline (naive mean + 3SDs). Values below the limit of detection were estimated to be at half the highest input dilution. The AUC was calculated in GraphPad Prism v.8.2.1 and represents the total peak area, where baseline was set as described above, with peaks <10% of the y axis minimum to maximum ignored. When AUC values could not be calculated, an arbitrary value of 1.0 was assigned.

Antibody-dependent cellular cytotoxicity assay

A reporter-based ADCC assay was performed according to the kit manufacturer's protocol (Promega, Madison, WI) with modifications. Briefly, cH6/1-expressing MDCK cells (MCDK-cH6/1)[63] were seeded at 2.5 × 10^4 cells/well in sterile white 96-well plates (Costar) in complete 1× MEM and incubated at 37°C with 5% CO_2. In a separate assay, MDCK cells were seeded as above but were infected overnight at 37°C with a multiplicity of infection (MOI) 5 of H5N1 in a final volume of 100 μL UltraMDCK media. After 24 h or 48 h, media and virus suspension was removed from

Please cite this article in press as: Bliss et al., A single-shot adenoviral vaccine provides hemagglutinin stalk-mediated protection against heterosubtypic influenza challenge in mice, Molecular Therapy (2022), https://doi.org/10.1016/j.ymthe.2022.01.011

MDCK-cH6/1 cells or H5N1-infected MDCKs, respectively, and 25 μL pre-warmed RPMI 1640 (Gibco, Gaithersburg, MD) media added per well. In a separate plate, pooled mouse serum was diluted 1:10 in cold RPMI and a 3-fold serial dilution performed, and then, 25 μL of diluted mouse serum was added to the MDCK cells. A stable Jurkat cell line expressing mouse FcγRIV (Promega, Madison, WI) was rapidly thawed and reconstituted in pre-warmed RPMI media and then added to MDCK-cH6/1- or MDCK-H5N1-infected cells in a 25 μL volume at an effector-to-target-cell ratio of approximately 1.7–2.5:1. After 6 h at 37°C with 5% CO_2, cells were equilibrated to room temperature for 15 min and then 75 μL Bio-Glo Luciferase assay substrate (Promega, Madison, WI) was added. Luminescence was immediately read using a Synergy H1 hybrid multimode microplate reader (BioTek Instruments). For AUC analysis, background subtracted relative light units (RLUs) were used to define the area, using mean plus 3SDs of negative control wells (no Ab wells) as the defined baseline. Alternatively, background subtracted raw RLUs were plotted (Figures S4J and S4L).

Hemagglutination inhibition assay

Mouse serum was incubated overnight in a 37°C water bath in the presence of receptor-destroying enzyme (RDE) and then resuspended in 2.5% sodium citrate and heated for 30 min in a 56°C water bath. RDE-treated serum samples were then diluted to 1:10 of original serum volume in PBS and tested by standard HI assay. Briefly, turkey red blood cells (RBCs) were mixed 1:1 in PBS and then washed in a benchtop microcentrifuge at 2,000 rpm for 2 min. Supernatant was removed and a 0.5% RBC solution prepared by dilution in PBS. A/Netherlands/602/2009(pH1N1) virus was diluted to 160 hemagglutination activity units (HAUs)/mL, determined by HA assay, in PBS. In V-bottom 96-well plates, 50 μL of RDE-treated serum was 2-fold serially diluted in 25 μL of PBS. Four HAUs of pH1N1 virus in 25 μL was added to each well and the plates gently agitated. Plates were incubated for 30 min at room temperature and then 50 μL of 0.5% turkey RBCs was added. Plates were incubated at 4°C for 45 min. The hemagglutination inhibition (HI) titers were determined by the last well in which hemagglutination of RBC did not occur.

Quantification of lung viral titers

Following euthanasia, whole lungs were harvested, trimmed, and the entire lung placed into BeadBug tubes containing 3-mm beads and pre-filled with 1 mL of sterile PBS (Sigma-Aldrich, St. Louis, MO). Tubes were kept on ice until homogenization in a BeadBlaster (Benchmark Scientific, Sayreville, NJ) using the following settings for two cycles: 6 m/s; 20 s shaking; and 20-s intervals. Tubes were removed and pelleted at maximum speed in a benchtop centrifuge pre-chilled to 4°C. The cleared lysate was aliquoted into fresh tubes and stored at −80°C until ready for quantification of viral lung titers using an immunostaining-based plaque assay.

MDCK cells were seeded in 12-well plates at 0.4×10^6 cells/well in a final volume of 1 mL. The following day, aliquots of lung homogenates were thawed and serially diluted 10-fold in infection medium (1× PBS with 100 μg/mL penicillin-streptomycin, 0.2% BSA, 0.83 mM $CaCl_2$, and 1 mM of $MgCl_2$). Single-use aliquots for a stock of H1N1 virus of known titer were included to act as a positive control between assays. MDCK cells were washed once with 1 mL pre-warmed PBS and the suspension replaced with 250 μL of each experimental sample and corresponding dilutions. Virus suspension was allowed to absorb to cells for 1 h at 37°C with gentle rocking every 15 min to ensure even distribution of the suspension. Following incubation, the cells were washed with PBS and overlaid with 1 mL overlay medium. Overlay medium consists of an equal volume of 2× agar solution (0.02% DEAE-dextran, 0.2% sodium bicarbonate, 2 μg/mL of TPCK-treated trypsin, and 1.2% Oxoid agar in water for injection [WFI]) added to 2× MEM (Gibco) containing 4 mM L-glutamine, 0.24% sodium bicarbonate, 20 mM 4-HEPES, 200 μg/mL penicillin-streptomycin, and 0.42% BSA. Cells were then incubated for 42–44 h at 37°C until visible plaques were observed. Cells were fixed for at least 2 h in 4% formaldehyde and plaques immunostained for 2 h at room temperature with HA-stalk-specific human mAb CR9114 diluted in 1% dry milk to a final concentration of 0.41 μg/mL. Following primary Ab incubation, cells were stained for 1 h with goat anti-human IgG conjugated to HRP (Sigma-Millipore) at a final dilution of 1:5,000 in 1% dry milk. Cells were washed with tap water and 500 μL TrueBlue peroxidase substrate (SeraCare Life Sciences, Gaithersburg, MD) added per well and allowed to incubate for 10–15 min. Plaques were counted in wells that had 10–100 plaques and titer calculated for each lung homogenate sample as PFUs/mL as follows: dilution of well × number of plaques and adjusted for virus volume added per well. Quality control (QC) by microscopy ensured monolayer was intact.

Lung histology and pathological evaluation

Lungs were harvested following influenza virus challenge at the time of euthanasia or, in the case of survival, at the end of the experiment on D14 post-challenge. Lungs were inflated with 10% formalin and submitted to the Biorepository and Pathology Core at ISMMS for tissue processing and paraffin embedding. Lung-tissue sections 5 μm in thickness were stained using H&E and evaluated by a veterinary pathologist who was blinded to the treatment groups, with the exception of the PBS vaccinated + challenge and PBS mock challenge group. Images were captured under 200× magnification using an Olympus B×43 with an Olympus DP21 Digital Camera system.

Flow cytometry and data analysis

FACS data were acquired on an LSRII cytometer (BD Biosciences, Franklin Lakes, NJ), FACSDiva v.7.03 (BD Biosciences, Franklin Lakes, NJ), with photon multiplier tube voltages set by daily acquisition of Cytometer Setup and Tracking beads (BD Biosciences, Franklin Lakes, NJ). Flow cytometry standard (FCS) files were analyzed using FlowJo v.10.4.2 (Treestar, Ashland, OR). A sample gating strategy is provided in Figure S6 for intracellular cytokine staining. Compensation was calculated in FlowJo, based on single fluorochrome compensation bead controls.

For intracellular cytokine staining, greater than 12,900 $CD4^+$ and >1,800 $CD8^+$ PBMCs were acquired on test samples and >36,700

$CD4^+$ and >17,400 $CD8^+$ cells acquired per splenocyte test sample. Data were analyzed using FlowJo v.10.4.2 (Treestar, Ashland, OR), gating on lymphocytes, singlets, live cells, $CD3^+$, $CD4^+$, or $CD8^+$ and then assessed for IFN-γ, IL-2, TNF-α, and CD40L responses and for CD107a expression. Responses in autologous DMSO negative controls were subtracted from HA stalk-stimulated and PMA/ionomycin stimulated responses, with HA-stalk-specific responses reported as frequency of positive cells per parent $CD4^+$ or $CD8^+$ T cell population. All PMA/ionomycin stimulated splenocytes passed a >1% cytokine response threshold. Representative PMA/ionomycin stimulated PBMC samples (n = 3 per run) passed a >1% cytokine response threshold for ≥ 2 cytokines.

Statistical analyses

Differences between Ad5_H1-vaccinated groups compared with relevant controls (i.e., conventional H1N1 IIV or irrelevant antigen vaccine Ad5_EGFP) were calculated using a Kruskal-Wallis test with Dunn's correction for multiple comparisons. Comparisons between two groups were performed using a non-parametric Mann-Whitney test. Survival was determined using a Kaplan-Meier survival curve and significance thresholds calculated using Mantel-Cox log rank test, manually corrected for multiple comparisons against the relevant comparator using Bonferroni method. Statistical significance was determined to be $^*p < 0.05$, $^{**}p < 0.01$, $^{***}p < 0.001$, or $^{****}p < 0.0001$. Data were graphed using GraphPad Prism v.8.2.1 (GraphPad Software, CA, USA).

SUPPLEMENTAL INFORMATION

Supplemental information can be found online at https://doi.org/10.1016/j.ymthe.2022.01.011.

ACKNOWLEDGMENTS

We would like to thank Dr. Alison Turner and Louisa Rose at The Jenner Institute's Viral Vector Core Facility for assistance in generating recombinant adenoviral vectors. We thank Dr. Carole Henry and Dr. Patrick Wilson (University of Chicago) for providing plasmids to express CR9114 and FI6 mAbs. We would like to acknowledge the members of the Flow Cytometry Core and The Center for Comparative Medicine and Surgery (CCMS) at the Icahn School of Medicine at Mount Sinai (ISMMS), in addition to Chen Wang, the Palese laboratory manager at ISMMS. This research project was supported in part by funding from NIH/NIAID 1R21AI146529 (L.C.) and NIH/NIAID CEIRS HHSN272201400008C (L.C., P.P., and F.K.) and the CEIRS Training Program (HHSN272201400008C). The work was also partially funded by NIAID grant P01 AI097092-07 (P.P.), NIAID grant R01 AI145870-03 (P.P.), and the NIAID Collaborative Influenza Vaccine Innovation Centers (CIVIC) contract 75N93019C00051 (P.P., F.K., and W.S.). L.C. was funded by the HC Roscoe Grant 2016 from the British Medical Association (BMA) Foundation for Medical Research, and the US Graduate Women in Science (GWIS) 2017 Nell Mondy and Monique Braude Fellowship. Figures were created with BioRender—biorender.com. Work was performed at Icahn School of Medicine at Mount Sinai (ISMMS), New York, NY 10029, USA.

AUTHOR CONTRIBUTIONS

Conceptualization, L.C.; methodology, C.M.B., A.W.F., R.N., W.S., M.M., and L.C.; validation, C.M.B. and L.C.; formal analysis, A.W.F., C.M.B., V.L.G., and L.C.; investigation, C.M.B., A.W.F., W.S., T.G.C., V.L.G., V.H.L.-G., and L.C.; resources, R.N., G.S.T., M.M., F.K., A.V.S.H., P.P., and L.C.; writing – original draft, C.M.B. and L.C.; writing – review and editing, all authors contributed to review and editing of the final draft; visualization, C.M.B. and L.C.; supervision, L.C.; funding acquisition, P.P. and L.C.

DECLARATION OF INTERESTS

The Icahn School of Medicine has submitted patents covering a universal influenza virus vaccine (P.P., W.S., and F.K.). A.V.S.H. is named as an inventor on a patent covering use of adenoviral vectored vaccines and is a co-founder of, consultant to, and shareholder in Vaccitech plc, which is developing adenoviral vectored vaccines. The remaining authors declare no competing interests.

REFERENCES

1. Palese, P. (2004). Influenza: old and new threats. Nat. Med. *10*, S82–S87. https://doi.org/10.1038/nm1141.
2. Kerstetter, L., Buckley, S., Bliss, C., and Coughlan, L. (2021). Adenoviral vectors as vaccines for emerging avian influenza viruses. Front. Immunol. *11*, 607333. https://doi.org/10.3389/fimmu.2020.607333.
3. Coughlan, L., and Palese, P. (2018). Overcoming barriers in the path to a universal influenza virus vaccine. Cell Host Microbe *24*, 18–24. https://doi.org/10.1016/j.chom.2018.06.016.
4. Pyankova, O.G., Susloparov, I.M., Moiseeva, A.A., Kolosova, N.P., Onkhonova, G.S., Danilenko, A.V., Vakalova, E.V., Shendo, G.L., Nekeshina, N.N., Noskova, L.N., and Demina, J.V. (2021). Isolation of clade 2.3.4.4b A(H5N8), a highly pathogenic avian influenza virus, from a worker during an outbreak on a poultry farm, Russia, December 2020. Euro Surveill. *26*, 2100439. https://doi.org/10.2807/1560-7917.ES.2021.26.24.2100439.
5. Angeletti, D., Kosik, I., Santos, J.J.S., Yewdell, W.T., Boudreau, C.M., Mallajosyula, V.V.A., Mankowski, M.C., Chambers, M., Prabhakaran, M., Hickman, H.D., and McDermott, A.B. (2019). Outflanking immunodominance to target subdominant broadly neutralizing epitopes. Proc. Natl. Acad. Sci. U S A *116*, 13474–13479. https://doi.org/10.1073/pnas.1816300116.
6. Tan, H.X., Jegaskanda, S., Juno, J.A., Esterbauer, R., Wong, J., Kelly, H.G., Liu, Y., Tilmanis, D., Hurt, A.C., Yewdell, J.W., and Kent, S.J. (2019). Subdominance and poor intrinsic immunogenicity limit humoral immunity targeting influenza HA stem. J. Clin. Invest. *129*, 850–862. https://doi.org/10.1172/JCI123366.
7. Heaton, N.S., Sachs, D., Chen, C.J., Hai, R., and Palese, P. (2013). Genome-wide mutagenesis of influenza virus reveals unique plasticity of the hemagglutinin and NS1 proteins. Proc. Natl. Acad. Sci. U S A *110*, 20248–20253. https://doi.org/10.1073/pnas.1320524110.
8. Doud, M.B., and Bloom, J.D. (2016). Accurate measurement of the effects of all amino-acid mutations on influenza hemagglutinin. Viruses *8*, 155. https://doi.org/10.3390/v8060155.
9. Doud, M.B., Lee, J.M., and Bloom, J.D. (2018). How single mutations affect viral escape from broad and narrow antibodies to H1 influenza hemagglutinin. Nat. Commun. *9*, 1386. https://doi.org/10.1038/s41467-018-03665-3.
10. Kirkpatrick, E., Qiu, X., Wilson, P.C., Bahl, J., and Krammer, F. (2018). The influenza virus hemagglutinin head evolves faster than the stalk domain. Sci. Rep. *8*, 10432. https://doi.org/10.1038/s41598-018-28706-1.
11. Flannery, B., Chung, J.R., Belongia, E.A., McLean, H.Q., Gaglani, M., Murthy, K., Zimmerman, R.K., Nowalk, M.P., Jackson, M.L., Jackson, L.A., and Monto, A.S. (2018). Interim estimates of 2017-18 seasonal influenza vaccine effectiveness - United States, February 2018. MMWR Morb. Mortal. Wkly. Rep. *67*, 180–185. https://doi.org/10.15585/mmwr.mm6706a2.

12. Skowronski, D.M., Chambers, C., De Serres, G., Dickinson, J.A., Winter, A.L., Hickman, R., Chan, T., Jassem, A.N., Drews, S.J., Charest, H., and Gubbay, J.B. (2018). Early season co-circulation of influenza A(H3N2) and B(Yamagata): interim estimates of 2017/18 vaccine effectiveness, Canada, January 2018. Euro Surveill. *23*. 18-00035. https://doi.org/10.2807/1560-7917.ES.2018.23.5.18-00035.

13. Sullivan, S.G., Chilver, M.B., Carville, K.S., Deng, Y.M., Grant, K.A., Higgins, G., Komadina, N., Leung, V.K., Minney-Smith, C.A., Teng, D., and Tran, T. (2017). Low interim influenza vaccine effectiveness, Australia, 1 May to 24 September 2017. Euro Surveill. *22*. 17-00707. https://doi.org/10.2807/1560-7917.ES.2017.22.43.17-00707.

14. Kissling, E., Rose, A., Emborg, H.D., Gherasim, A., Pebody, R., Pozo, F., Trebbien, R., Mazagatos, C., Whitaker, H., and Valenciano, M. (2019). Interim 2018/19 influenza vaccine effectiveness: six European studies, October 2018 to January 2019. Euro Surveill. *24*, 1900121. https://doi.org/10.2807/1560-7917.ES.2019.24.1900121.

15. Rose, A., Kissling, E., Emborg, H.D., Larrauri, A., McMenamin, J., Pozo, F., Trebbien, R., Mazagatos, C., Whitaker, H., and Valenciano, M. (2020). Interim 2019/20 influenza vaccine effectiveness: six European studies, September 2019 to January 2020. Euro Surveill. *25*, 2000153. https://doi.org/10.2807/1560-7917.ES.2020.25.10.2000153.

16. Gerdil, C. (2003). The annual production cycle for influenza vaccine. Vaccine *21*, 1776–1779. https://doi.org/10.1016/s0264-410x(03)00071-9.

17. Krammer, F., and Palese, P. (2014). Universal influenza virus vaccines: need for clinical trials. Nat. Immunol. *15*, 3–5. https://doi.org/10.1038/ni.2761.

18. Zost, S.J., Parkhouse, K., Gumina, M.E., Kim, K., Diaz Perez, S., Wilson, P.C., Treanor, J.J., Sant, A.J., Cobey, S., and Hensley, S.E. (2017). Contemporary H3N2 influenza viruses have a glycosylation site that alters binding of antibodies elicited by egg-adapted vaccine strains. Proc. Natl. Acad. Sci. U S A *114*, 12578–12583. https://doi.org/10.1073/pnas.1712377114.

19. Wu, N.C., Zost, S.J., Thompson, A.J., Oyen, D., Nycholat, C.M., McBride, R., Paulson, J.C., Hensley, S.E., and Wilson, I.A. (2017). A structural explanation for the low effectiveness of the seasonal influenza H3N2 vaccine. PLoS Pathog. *13*, e1006682. https://doi.org/10.1371/journal.ppat.1006682.

20. Garretson, T.A., Petrie, J.G., Martin, E.T., Monto, A.S., and Hensley, S.E. (2018). Identification of human vaccinees that possess antibodies targeting the egg-adapted hemagglutinin receptor binding site of an H1N1 influenza vaccine strain. Vaccine *36*, 4095–4101. https://doi.org/10.1016/j.vaccine.2018.05.086.

21. Steel, J., Lowen, A.C., Wang, T.T., Yondola, M., Gao, Q., Haye, K., García-Sastre, A., and Palese, P. (2010). Influenza virus vaccine based on the conserved hemagglutinin stalk domain. mBio *1*. e00018-10. https://doi.org/10.1128/mBio.00018-10.

22. Yassine, H.M., Boyington, J.C., McTamney, P.M., Wei, C.J., Kanekiyo, M., Kong, W.P., Gallagher, J.R., Wang, L., Zhang, Y., Joyce, M.G., and Lingwood, D. (2015). Hemagglutinin-stem nanoparticles generate heterosubtypic influenza protection. Nat. Med. *21*, 1065–1070. https://doi.org/10.1038/nm.3927.

23. Impagliazzo, A., Milder, F., Kuipers, H., Wagner, M.V., Zhu, X., Hoffman, R.M., van Meersbergen, R., Huizingh, J., Wanningen, P., Verspuij, J., and de Man, M. (2015). A stable trimeric influenza hemagglutinin stem as a broadly protective immunogen. Science *349*, 1301–1306. https://doi.org/10.1126/science.aac7263.

24. Valkenburg, S.A., Mallajosyula, V.V., Li, O.T., Chin, A.W., Carnell, G., Temperton, N., Varadarajan, R., and Poon, L.L. (2016). Stalking influenza by vaccination with pre-fusion headless HA mini-stem. Sci. Rep. *6*, 22666. https://doi.org/10.1038/srep22666.

25. Nachbagauer, R., Liu, W.C., Choi, A., Wohlbold, T.J., Atlas, T., Rajendran, M., Solórzano, A., Berlanda-Scorza, F., García-Sastre, A., Palese, P., and Albrecht, R.A. (2017). A universal influenza virus vaccine candidate confers protection against pandemic H1N1 infection in preclinical ferret studies. NPJ Vaccines *2*, 26. https://doi.org/10.1038/s41541-017-0026-4.

26. Nachbagauer, R., Kinzler, D., Choi, A., Hirsh, A., Beaulieu, E., Lecrenier, N., Innis, B.L., Palese, P., Mallett, C.P., and Krammer, F. (2016). A chimeric haemagglutinin-based influenza split virion vaccine adjuvanted with AS03 induces protective stalk-reactive antibodies in mice. NPJ Vaccines *1*, 16015. https://doi.org/10.1038/npjvaccines.2016.15.

27. Hai, R., Krammer, F., Tan, G.S., Pica, N., Eggink, D., Maamary, J., Margine, I., Albrecht, R.A., and Palese, P. (2012). Influenza viruses expressing chimeric hemagglutinins: globular head and stalk domains derived from different subtypes. J. Virol. *86*, 5774–5781. https://doi.org/10.1128/JVI.00137-12.

28. Bernstein, D.I., Guptill, J., Naficy, A., Nachbagauer, R., Berlanda-Scorza, F., Feser, J., Wilson, P.C., Solórzano, A., Van der Wielen, M., Walter, E.B., and Albrecht, R.A. (2020). Immunogenicity of chimeric haemagglutinin-based, universal influenza virus vaccine candidates: interim results of a randomised, placebo-controlled, phase 1 clinical trial. Lancet Infect. Dis. *20*, 80–91. https://doi.org/10.1016/S1473-3099(19)30393-7.

29. Nachbagauer, R., Feser, J., Naficy, A., Bernstein, D.I., Guptill, J., Walter, E.B., Berlanda-Scorza, F., Stadlbauer, D., Wilson, P.C., Aydillo, T., and Behzadi, M.A. (2021). A chimeric hemagglutinin-based universal influenza virus vaccine approach induces broad and long-lasting immunity in a randomized, placebo-controlled phase I trial. Nat. Med. *27*, 106–114. https://doi.org/10.1038/s41591-020-1118-7.

30. Ng, S., Nachbagauer, R., Balmaseda, A., Stadlbauer, D., Ojeda, S., Patel, M., Rajabhathor, A., Lopez, R., Guglia, A.F., Sanchez, N., and Amanat, F. (2019). Novel correlates of protection against pandemic H1N1 influenza A virus infection. Nat. Med. *25*, 962–967. https://doi.org/10.1038/s41591-019-0463-x.

31. Andrews, S.F., Huang, Y., Kaur, K., Popova, L.I., Ho, I.Y., Pauli, N.T., Dunand, C.J.H., Taylor, W.M., Lim, S., Huang, M., and Qu, X. (2015). Immune history profoundly affects broadly protective B cell responses to influenza. Sci. Transl. Med. *7*, 316ra192. https://doi.org/10.1126/scitranslmed.aad0522.

32. Tao, Y., Strelkov, S.V., Mesyanzhinov, V.V., and Rossmann, M.G. (1997). Structure of bacteriophage T4 fibritin: a segmented coiled coil and the role of the C-terminal domain. Structure *5*, 789–798. https://doi.org/10.1016/s0969-2126(97)00233-5.

33. Krammer, F., Margine, I., Tan, G.S., Pica, N., Krause, J.C., and Palese, P. (2012). A carboxy-terminal trimerization domain stabilizes conformational epitopes on the stalk domain of soluble recombinant hemagglutinin substrates. PLoS One *7*, e43603. https://doi.org/10.1371/journal.pone.0043603.

34. Dreyfus, C., Laursen, N.S., Kwaks, T., Zuijdgeest, D., Khayat, R., Ekiert, D.C., Lee, J.H., Metlagel, Z., Bujny, M.V., Jongeneelen, M., and Van Der Vlugt, R. (2012). Highly conserved protective epitopes on influenza B viruses. Science *337*, 1343–1348. https://doi.org/10.1126/science.1222908.

35. Corti, D., Voss, J., Gamblin, S.J., Codoni, G., Macagno, A., Jarrossay, D., Vachieri, S.G., Pinna, D., Minola, A., Vanzetta, F., and Silacci, C. (2011). A neutralizing antibody selected from plasma cells that binds to group 1 and group 2 influenza A hemagglutinins. Science *333*, 850–856. https://doi.org/10.1126/science.1205669.

36. Heaton, N.S., Leyva-Grado, V.H., Tan, G.S., Eggink, D., Hai, R., and Palese, P. (2013). In vivo bioluminescent imaging of influenza a virus infection and characterization of novel cross-protective monoclonal antibodies. J. Virol. *87*, 8272–8281. https://doi.org/10.1128/JVI.00969-13.

37. de Jong, J.C., Palache, A.M., Beyer, W.E., Rimmelzwaan, G.F., Boon, A.C., and Osterhaus, A.D. (2003). Haemagglutination-inhibiting antibody to influenza virus. Dev. Biol. (Basel) *115*, 63–73.

38. Hannoun, C., Megas, F., and Piercy, J. (2004). Immunogenicity and protective efficacy of influenza vaccination. Virus Res. *103*, 133–138. https://doi.org/10.1016/j.virusres.2004.02.025.

39. Hobson, D., Curry, R.L., Beare, A.S., and Ward-Gardner, A. (1972). The role of serum haemagglutination-inhibiting antibody in protection against challenge infection with influenza A2 and B viruses. J. Hyg. (Lond) *70*, 767–777. https://doi.org/10.1017/s0022172400022610.

40. Sridhar, S., Brokstad, K.A., and Cox, R.J. (2015). Influenza vaccination strategies: comparing inactivated and live attenuated influenza vaccines. Vaccines (Basel) *3*, 373–389. https://doi.org/10.3390/vaccines3020373.

41. Mohn, K.G., Brokstad, K.A., Islam, S., Oftung, F., Tondel, C., Aarstad, H.J., and Cox, R.J. (2020). Early induction of cross-reactive CD8+ T-cell responses in tonsils after live-attenuated influenza vaccination in children. J. Infect. Dis. *221*, 1528–1537. https://doi.org/10.1093/infdis/jiz583.

42. Zens, K.D., Chen, J.K., and Farber, D.L. (2016). Vaccine-generated lung tissue-resident memory T cells provide heterosubtypic protection to influenza infection. JCI Insight *1*, e85832. https://doi.org/10.1172/jci.insight.85832.

43. Clemens, E.B., van de Sandt, C., Wong, S.S., Wakim, L.M., and Valkenburg, S.A. (2018). Harnessing the power of T cells: the promising hope for a universal influenza vaccine. Vaccines (Basel) *6*, 18. https://doi.org/10.3390/vaccines6020018.

44. Miller, M.A., Ganesan, A.P., Luckashenak, N., Mendonca, M., and Eisenlohr, L.C. (2015). Endogenous antigen processing drives the primary CD4+ T cell response to influenza. Nat. Med. *21*, 1216–1222. https://doi.org/10.1038/nm.3958.

45. Tatsis, N., Fitzgerald, J.C., Reyes-Sandoval, A., Harris-McCoy, K.C., Hensley, S.E., Zhou, D., Lin, S.W., Bian, A., Xiang, Z.Q., Iparraguirre, A., and Lopez-Camacho, C. (2007). Adenoviral vectors persist in vivo and maintain activated CD8+ T cells: implications for their use as vaccines. Blood *110*, 1916–1923. https://doi.org/10.1182/blood-2007-02-062117.

46. Bliss, C.M., Parsons, A.J., Nachbagauer, R., Hamilton, J.R., Cappuccini, F., Ulaszewska, M., Webber, J.P., Clayton, A., Hill, A.V., and Coughlan, L. (2020). Targeting antigen to the surface of EVs improves the in vivo immunogenicity of human and non-human adenoviral vaccines in mice. Mol. Ther. Methods Clin. Dev. *16*, 108–125. https://doi.org/10.1016/j.omtm.2019.12.003.

47. Fitzgerald, J.C., Gao, G.P., Reyes-Sandoval, A., Pavlakis, G.N., Xiang, Z.Q., Wlazlo, A.P., Giles-Davis, W., Wilson, J.M., and Ertl, H.C. (2003). A simian replication-defective adenoviral recombinant vaccine to HIV-1 gag. J. Immunol. *170*, 1416–1422. https://doi.org/10.4049/jimmunol.170.3.1416.

48. Penaloza-MacMaster, P., Provine, N.M., Ra, J., Borducchi, E.N., McNally, A., Simmons, N.L., Iampietro, M.J., and Barouch, D.H. (2013). Alternative serotype adenovirus vaccine vectors elicit memory T cells with enhanced anamnestic capacity compared to Ad5 vectors. J. Virol. *87*, 1373–1384. https://doi.org/10.1128/JVI.02058-12.

49. Tan, W.G., Jin, H.T., West, E.E., Penaloza-MacMaster, P., Wieland, A., Zilliox, M.J., McElrath, M.J., Barouch, D.H., and Ahmed, R. (2013). Comparative analysis of simian immunodeficiency virus gag-specific effector and memory CD8+ T cells induced by different adenovirus vectors. J. Virol. *87*, 1359–1372. https://doi.org/10.1128/JVI.02055-12.

50. Quinn, K.M., Da Costa, A., Yamamoto, A., Berry, D., Lindsay, R.W., Darrah, P.A., Wang, L., Cheng, C., Kong, W.P., Gall, J.G., and Nicosia, A. (2013). Comparative analysis of the magnitude, quality, phenotype, and protective capacity of simian immunodeficiency virus gag-specific CD8+ T cells following human-, simian-, and chimpanzee-derived recombinant adenoviral vector immunization. J. Immunol. *190*, 2720–2735. https://doi.org/10.4049/jimmunol.1202861.

51. Crotty, S. (2015). A brief history of T cell help to B cells. Nat. Rev. Immunol. *15*, 185–189. https://doi.org/10.1038/nri3803.

52. Chen, H., Xiang, Z.Q., Li, Y., Kurupati, R.K., Jia, B., Bian, A., Zhou, D.M., Hutnick, N., Yuan, S., Gray, C., and Serwanga, J. (2010). Adenovirus-based vaccines: comparison of vectors from three species of adenoviridae. J. Virol. *84*, 10522–10532. https://doi.org/10.1128/JVI.00450-10.

53. Leon, P.E., He, W., Mullarkey, C.E., Bailey, M.J., Miller, M.S., Krammer, F., Palese, P., and Tan, G.S. (2016). Optimal activation of Fc-mediated effector functions by influenza virus hemagglutinin antibodies requires two points of contact. Proc. Natl. Acad. Sci. U S A *113*, E5944–E5951. https://doi.org/10.1073/pnas.1613225113.

54. DiLillo, D.J., Palese, P., Wilson, P.C., and Ravetch, J.V. (2016). Broadly neutralizing anti-influenza antibodies require Fc receptor engagement for in vivo protection. J. Clin. Invest. *126*, 605–610. https://doi.org/10.1172/JCI84428.

55. DiLillo, D.J., Tan, G.S., Palese, P., and Ravetch, J.V. (2014). Broadly neutralizing hemagglutinin stalk-specific antibodies require FcgammaR interactions for protection against influenza virus in vivo. Nat. Med. *20*, 143–151. https://doi.org/10.1038/nm.3443.

56. He, W., Chen, C.J., Mullarkey, C.E., Hamilton, J.R., Wong, C.K., Leon, P.E., Uccellini, M.B., Chromikova, V., Henry, C., Hoffman, K.W., and Lim, J.K. (2017). Alveolar macrophages are critical for broadly-reactive antibody-mediated protection against influenza A virus in mice. Nat. Commun. *8*, 846. https://doi.org/10.1038/s41467-017-00928-3.

57. Guthmiller, J.J., Han, J., Utset, H.A., Li, L., Lan, L.Y., Henry, C., Stamper, C.T., McMahon, M., O'Dell, G., Fernández-Quintero, M.L., and Freyn, A.W. (2021). Broadly neutralizing antibodies target a hemagglutinin anchor epitope. Nature, 1–10. https://doi.org/10.1038/s41586-021-04356-8.

58. Choi, A., Bouzya, B., Cortes Franco, K.D., Stadlbauer, D., Rajabhathor, A., Rouxel, R.N., Mainil, R., Van der Wielen, M., Palese, P., García-Sastre, A., and Innis, B.L. (2019). Chimeric hemagglutinin-based influenza virus vaccines induce protective stalk-specific humoral immunity and cellular responses in mice. Immunohorizons *3*, 133–148. https://doi.org/10.4049/immunohorizons.1900022.

59. Paules, C.I., Lakdawala, S., McAuliffe, J.M., Paskel, M., Vogel, L., Kallewaard, N.L., Zhu, Q., and Subbarao, K. (2017). The hemagglutinin A stem antibody MEDI8852 prevents and controls disease and limits transmission of pandemic influenza viruses. J. Infect. Dis. *216*, 356–365. https://doi.org/10.1093/infdis/jix292.

60. Sutton, T.C., Lamirande, E.W., Bock, K.W., Moore, I.N., Koudstaal, W., Rehman, M., Weverling, G.J., Goudsmit, J., and Subbarao, K. (2017). In vitro neutralization is not predictive of prophylactic efficacy of broadly neutralizing monoclonal antibodies CR6261 and CR9114 against lethal H2 influenza virus challenge in mice. J. Virol. *91*. e01603-17. https://doi.org/10.1128/JVI.01603-17.

61. Ermler, M.E., Kirkpatrick, E., Sun, W., Hai, R., Amanat, F., Chromikova, V., Palese, P., and Krammer, F. (2017). Chimeric hemagglutinin constructs induce broad protection against influenza B virus challenge in the mouse model. J. Virol. *91*. e00286-17. https://doi.org/10.1128/JVI.00286-17.

62. Kavian, N., Hachim, A., Poon, L.L.M., and Valkenburg, S.A. (2020). Vaccination with ADCC activating HA peptide epitopes provides partial protection from influenza infection. Vaccine *38*, 5885–5890. https://doi.org/10.1016/j.vaccine.2020.07.008.

63. Chromikova, V., Tan, J., Aslam, S., Rajabhathor, A., Bermudez-Gonzalez, M., Ayllon, J., Simon, V., García-Sastre, A., Salaun, B., Nachbagauer, R., and Krammer, F. (2020). Activity of human serum antibodies in an influenza virus hemagglutinin stalk-based ADCC reporter assay correlates with activity in a CD107a degranulation assay. Vaccine *38*, 1953–1961. https://doi.org/10.1016/j.vaccine.2020.01.008.

64. Bruhns, P. (2012). Properties of mouse and human IgG receptors and their contribution to disease models. Blood *119*, 5640–5649. https://doi.org/10.1182/blood-2012-01-380121.

65. Bruhns, P., and Jonsson, F. (2015). Mouse and human FcR effector functions. Immunol. Rev. *268*, 25–51.

66. Harbury, P.B., Kim, P.S., and Alber, T. (1994). Crystal structure of an isoleucine-zipper trimer. Nature *371*, 80–83.

67. Tatsis, N., and Ertl, H.C. (2004). Adenoviruses as vaccine vectors. Mol. Ther. *10*, 616–629. https://doi.org/10.1016/j.ymthe.2004.07.013.

68. Xu, T., Qiao, J., Zhao, L., Wang, G., He, G., Li, K., Tian, Y., Gao, M., Wang, J., Wang, H., and Dong, C. (2006). Acute respiratory distress syndrome induced by avian influenza A (H5N1) virus in mice. Am. J. Respir. Crit. Care Med. *174*, 1011–1017. https://doi.org/10.1164/rccm.200511-1751OC.

69. Paules, C.I., Marston, H.D., Eisinger, R.W., Baltimore, D., and Fauci, A.S. (2017). The pathway to a universal influenza vaccine. Immunity *47*, 599–603. https://doi.org/10.1016/j.immuni.2017.09.007.

70. Colloca, S., Barnes, E., Folgori, A., Ammendola, V., Capone, S., Cirillo, A., Siani, L., Naddeo, M., Grazioli, F., Esposito, M.L., and Ambrosio, M. (2012). Vaccine vectors derived from a large collection of simian adenoviruses induce potent cellular immunity across multiple species. Sci. Transl. Med. *4*, 115ra112. https://doi.org/10.1126/scitranslmed.3002925.

71. Dicks, M.D., Guzman, E., Spencer, A.J., Gilbert, S.C., Charleston, B., Hill, A.V., and Cottingham, M.G. (2015). The relative magnitude of transgene-specific adaptive immune responses induced by human and chimpanzee adenovirus vectors differs between laboratory animals and a target species. Vaccine *33*, 1121–1128. https://doi.org/10.1016/j.vaccine.2015.01.042.

72. Antrobus, R.D., Coughlan, L., Berthoud, T.K., Dicks, M.D., Hill, A.V., Lambe, T., and Gilbert, S.C. (2014). Clinical assessment of a novel recombinant simian adenovirus ChAdOx1 as a vectored vaccine expressing conserved Influenza A antigens. Mol. Ther. *22*, 668–674. https://doi.org/10.1038/mt.2013.284.

73. Barouch, D.H., Tomaka, F.L., Wegmann, F., Stieh, D.J., Alter, G., Robb, M.L., Michael, N.L., Peter, L., Nkolola, J.P., Borducchi, E.N., and Chandrashekar, A. (2018). Evaluation of a mosaic HIV-1 vaccine in a multicentre, randomised, double-blind, placebo-controlled, phase 1/2a clinical trial (APPROACH) and in rhesus monkeys (NHP 13-19). Lancet *392*, 232–243. https://doi.org/10.1016/S0140-6736(18)31364-3.

74. Coughlan, L., Sridhar, S., Payne, R., Edmans, M., Milicic, A., Venkatraman, N., Lugonja, B., Clifton, L., Qi, C., Folegatti, P.M., and Lawrie, A.M. (2018). Heterologous two-dose vaccination with simian adenovirus and poxvirus vectors

elicits long-lasting cellular immunity to influenza virus A in healthy adults. EBioMedicine *29*, 146–154. https://doi.org/10.1016/j.ebiom.2018.02.011.

75. Bliss, C.M., Drammeh, A., Bowyer, G., Sanou, G.S., Jagne, Y.J., Ouedraogo, O., Edwards, N.J., Tarama, C., Ouedraogo, N., Ouedraogo, M., and Njie-Jobe, J. (2017). Viral vector malaria vaccines induce high-level T cell and antibody responses in west African children and infants. Mol. Ther. *25*, 547–559. https://doi.org/10.1016/j.ymthe.2016.11.003.

76. Ewer, K.J., Barrett, J.R., Belij-Rammerstorfer, S., Sharpe, H., Makinson, R., Morter, R., Flaxman, A., Wright, D., Bellamy, D., Bittaye, M., and Dold, C. (2021). T cell and antibody responses induced by a single dose of ChAdOx1 nCoV-19 (AZD1222) vaccine in a phase 1/2 clinical trial. Nat. Med. *27*, 270–278. https://doi.org/10.1038/s41591-020-01194-5.

77. Sadoff, J., Le Gars, M., Shukarev, G., Heerwegh, D., Truyers, C., de Groot, A.M., Stoop, J., Tete, S., Van Damme, W., Leroux-Roels, I., and Berghmans, P.J. (2021). Interim results of a phase 1-2a trial of Ad26.COV2.S Covid-19 vaccine. N. Engl. J. Med. *384*, 1824–1835. https://doi.org/10.1056/NEJMoa2034201.

78. Logunov, D.Y., Dolzhikova, I.V., Shcheblyakov, D.V., Tukhvatulin, A.I., Zubkova, O.V., Dzharullaeva, A.S., Kovyrshina, A.V., Lubenets, N.L., Grousova, D.M., Erokhova, A.S., and Botikov, A.G. (2021). Safety and efficacy of an rAd26 and rAd5 vector-based heterologous prime-boost COVID-19 vaccine: an interim analysis of a randomised controlled phase 3 trial in Russia. Lancet *397*, 671–681. https://doi.org/10.1016/S0140-6736(21)00234-8.

79. Ramasamy, M.N., Minassian, A.M., Ewer, K.J., Flaxman, A.L., Folegatti, P.M., Owens, D.R., Voysey, M., Aley, P.K., Angus, B., Babbage, G., and Belij-Rammerstorfer, S. (2021). Safety and immunogenicity of ChAdOx1 nCoV-19 vaccine administered in a prime-boost regimen in young and old adults (COV002): a single-blind, randomised, controlled, phase 2/3 trial. Lancet *396*, 1979–1993. https://doi.org/10.1016/S0140-6736(20)32466-1.

80. Afkhami, S., LeClair, D.A., Haddadi, S., Lai, R., Toniolo, S.P., Ertl, H.C., Cranston, E.D., Thompson, M.R., and Xing, Z. (2017). Spray dried human and chimpanzee adenoviral-vectored vaccines are thermally stable and immunogenic in vivo. Vaccine *35*, 2916–2924. https://doi.org/10.1016/j.vaccine.2017.04.026.

81. Alcock, R., Cottingham, M.G., Rollier, C.S., Furze, J., De Costa, S.D., Hanlon, M., Spencer, A.J., Honeycutt, J.D., Wyllie, D.H., Gilbert, S.C., and Bregu, M. (2010). Long-term thermostabilization of live poxviral and adenoviral vaccine vectors at supraphysiological temperatures in carbohydrate glass. Sci. Transl. Med. *2*, 19ra12. https://doi.org/10.1126/scitranslmed.3000490.

82. Wang, C., Dulal, P., Zhou, X., Xiang, Z., Goharriz, H., Banyard, A., Green, N., Brunner, L., Ventura, R., Collin, N., and Draper, S.J. (2018). A simian-adenovirus-vectored rabies vaccine suitable for thermostabilisation and clinical development for low-cost single-dose pre-exposure prophylaxis. PLoS Negl. Trop. Dis. *12*, e0006870. https://doi.org/10.1371/journal.pntd.0006870.

83. Croyle, M.A., Cheng, X., and Wilson, J.M. (2001). Development of formulations that enhance physical stability of viral vectors for gene therapy. Gene Ther. *8*, 1281–1290. https://doi.org/10.1038/sj.gt.3301527.

84. Capelle, M.A.H., Babich, L., van Deventer-Troost, J.P.E., Salerno, D., Krijgsman, K., Dirmeier, U., Raaby, B., and Adriaansen, J. (2018). Stability and suitability for storage and distribution of Ad26.ZEBOV/MVA-BN(R)-Filo heterologous prime-boost Ebola vaccine. Eur. J. Pharm. Biopharm. *129*, 215–221. https://doi.org/10.1016/j.ejpb.2018.06.001.

85. Asthagiri Arunkumar, G., McMahon, M., Pavot, V., Aramouni, M., Ioannou, A., Lambe, T., Gilbert, S., and Krammer, F. (2019). Vaccination with viral vectors expressing NP, M1 and chimeric hemagglutinin induces broad protection against influenza virus challenge in mice. Vaccine *37*, 5567–5577. https://doi.org/10.1016/j.vaccine.2019.07.095.

86. McMahon, M., Asthagiri Arunkumar, G., Liu, W.C., Stadlbauer, D., Albrecht, R.A., Pavot, V., Aramouni, M., Lambe, T., Gilbert, S.C., and Krammer, F. (2019). Vaccination with viral vectors expressing chimeric hemagglutinin, NP and M1 antigens protects ferrets against influenza virus challenge. Front. Immunol. *10*, 2005. https://doi.org/10.3389/fimmu.2019.02005.

87. Yamada, S., Yasuhara, A., and Kawaoka, Y. (2019). Soluble recombinant hemagglutinin protein of H1N1pdm09 influenza virus elicits cross-protection against a lethal H5N1 challenge in mice. Front. Microbiol. *10*, 2031. https://doi.org/10.3389/fmicb.2019.02031.

88. Krammer, F., Pica, N., Hai, R., Margine, I., and Palese, P. (2013). Chimeric hemagglutinin influenza virus vaccine constructs elicit broadly protective stalk-specific antibodies. J. Virol. *87*, 6542–6550. https://doi.org/10.1128/JVI.00641-13.

89. Tapia, M.D., Sow, S.O., Lyke, K.E., Haidara, F.C., Diallo, F., Doumbia, M., Traore, A., Coulibaly, F., Kodio, M., Onwuchekwa, U., and Sztein, M.B. (2016). Use of Chad3-EBO-Z Ebola virus vaccine in Malian and US adults, and boosting of Malian adults with MVA-BN-Filo: a phase 1, single-blind, randomised trial, a phase 1b, open-label and double-blind, dose-escalation trial, and a nested, randomised, double-blind, placebo-controlled trial. Lancet Infect. Dis. *16*, 31–42. https://doi.org/10.1016/S1473-3099(15)00362-X.

90. de Barra, E., Hodgson, S.H., Ewer, K.J., Bliss, C.M., Hennigan, K., Collins, A., Berrie, E., Lawrie, A.M., Gilbert, S.C., Nicosia, A., and McConkey, S.J. (2014). A phase Ia study to assess the safety and immunogenicity of new malaria vaccine candidates Chad63 CS administered alone and with MVA CS. PLoS One *9*, e115161. https://doi.org/10.1371/journal.pone.0115161.

91. Tan, G.S., Leon, P.E., Albrecht, R.A., Margine, I., Hirsh, A., Bahl, J., and Krammer, F. (2016). Broadly-reactive neutralizing and non-neutralizing antibodies directed against the H7 influenza virus hemagglutinin reveal divergent mechanisms of protection. PLoS Pathog. *12*, e1005578. https://doi.org/10.1371/journal.ppat.1005578.

92. Henry Dunand, C.J., Leon, P.E., Huang, M., Choi, A., Chromikova, V., Ho, I.Y., Tan, G.S., Cruz, J., Hirsh, A., Zheng, N.Y., and Mullarkey, C.E. (2016). Both neutralizing and non-neutralizing human H7N9 influenza vaccine-induced monoclonal antibodies confer protection. Cell Host Microbe *19*, 800–813. https://doi.org/10.1016/j.chom.2016.05.014.

93. Huber, V.C., Lynch, J.M., Bucher, D.J., Le, J., and Metzger, D.W. (2001). Fc receptor-mediated phagocytosis makes a significant contribution to clearance of influenza virus infections. J. Immunol. *166*, 7381–7388. https://doi.org/10.4049/jimmunol.166.12.7381.

94. Lu, I.N., Farinelle, S., Sausy, A., and Muller, C.P. (2017). Identification of a CD4 T-cell epitope in the hemagglutinin stalk domain of pandemic H1N1 influenza virus and its antigen-driven TCR usage signature in BALB/c mice. Cell. Mol. Immunol. *14*, 511–520. https://doi.org/10.1038/cmi.2016.20.

95. Knowlden, Z.A.G., Richards, K.A., Moritzky, S.A., and Sant, A.J. (2019). Peptide epitope hot spots of CD4 T cell recognition within influenza hemagglutinin during the primary response to infection. Pathogens *8*, 220. https://doi.org/10.3390/pathogens8040220.

96. Rattan, A., Richards, K.A., Knowlden, Z.A.G., and Sant, A.J. (2019). Protein vaccination directs the CD4(+) T cell response toward shared protective epitopes that can be recalled after influenza virus infection. J. Virol. *93*. e00947-19. https://doi.org/10.1128/JVI.00947-19.

97. Wilkinson, T.M., Li, C.K., Chui, C.S., Huang, A.K., Perkins, M., Liebner, J.C., Lambkin-Williams, R., Gilbert, A., Oxford, J., Nicholas, B., and Staples, K.J. (2012). Preexisting influenza-specific CD4+ T cells correlate with disease protection against influenza challenge in humans. Nat. Med. *18*, 274–280. https://doi.org/10.1038/nm.2612.

98. Brown, D.M., Lee, S., Garcia-Hernandez Mde, L., and Swain, S.L. (2012). Multifunctional CD4 cells expressing gamma interferon and perforin mediate protection against lethal influenza virus infection. J. Virol. *86*, 6792–6803. https://doi.org/10.1128/JVI.07172-11.

99. Nayak, J.L., Richards, K.A., Yang, H., Treanor, J.J., and Sant, A.J. (2015). Effect of influenza A(H5N1) vaccine prepandemic priming on CD4+ T-cell responses. J. Infect. Dis. *211*, 1408–1417. https://doi.org/10.1093/infdis/jiu616.

100. Atsmon, J., Kate-Ilovitz, E., Shaikevich, D., Singer, Y., Volokhov, I., Haim, K.Y., and Ben-Yedidia, T. (2012). Safety and immunogenicity of multimeric-001–a novel universal influenza vaccine. J. Clin. Immunol. *32*, 595–603. https://doi.org/10.1007/s10875-011-9632-5.

101. McKinstry, K.K., Strutt, T.M., Kuang, Y., Brown, D.M., Sell, S., Dutton, R.W., and Swain, S.L. (2012). Memory CD4+ T cells protect against influenza through multiple synergizing mechanisms. J. Clin. Invest. *122*, 2847–2856. https://doi.org/10.1172/JCI63689.

102. Laidlaw, B.J., Decman, V., Ali, M.A., Abt, M.C., Wolf, A.I., Monticelli, L.A., Mozdzanowska, K., Angelosanto, J.M., Artis, D., Erikson, J., and Wherry, E.J. (2013). Cooperativity between CD8+ T cells, non-neutralizing antibodies, and

alveolar macrophages is important for heterosubtypic influenza virus immunity. PLoS Pathog. *9*, e1003207. https://doi.org/10.1371/journal.ppat.1003207.

103. Hayward, A.C., Wang, L., Goonetilleke, N., Fragaszy, E.B., Bermingham, A., Copas, A., Dukes, O., Millett, E.R., Nazareth, I., Nguyen-Van-Tam, J.S., and Watson, J.M. (2015). Natural T cell-mediated protection against seasonal and pandemic influenza. Results of the flu watch cohort study. Am. J. Respir. Crit. Care Med. *191*, 1422–1431. https://doi.org/10.1164/rccm.201411-1988OC.

104. Epstein, S.L., Kong, W.P., Misplon, J.A., Lo, C.Y., Tumpey, T.M., Xu, L., and Nabel, G.J. (2005). Protection against multiple influenza A subtypes by vaccination with highly conserved nucleoprotein. Vaccine *23*, 5404–5410. https://doi.org/10.1016/j.vaccine.2005.04.047.

105. Taylor, P.M., and Askonas, B.A. (1986). Influenza nucleoprotein-specific cytotoxic T-cell clones are protective in vivo. Immunology *58*, 417–420.

106. Coughlan, L. (2020). Factors which contribute to the immunogenicity of non-replicating adenoviral vectored vaccines. Front. Immunol. *11*, 909. https://doi.org/10.3389/fimmu.2020.00909.

107. Muruve, D.A., Petrilli, V., Zaiss, A.K., White, L.R., Clark, S.A., Ross, P.J., Parks, R.J., and Tschopp, J. (2008). The inflammasome recognizes cytosolic microbial and host DNA and triggers an innate immune response. Nature *452*, 103–107. https://doi.org/10.1038/nature06664.

108. Rhee, E.G., Blattman, J.N., Kasturi, S.P., Kelley, R.P., Kaufman, D.R., Lynch, D.M., La Porte, A., Simmons, N.L., Clark, S.L., Pulendran, B., and Greenberg, P.D. (2011). Multiple innate immune pathways contribute to the immunogenicity of recombinant adenovirus vaccine vectors. J. Virol. *85*, 315–323. https://doi.org/10.1128/JVI.01597-10.

109. Nakayama, T. (2016). An inflammatory response is essential for the development of adaptive immunity-immunogenicity and immunotoxicity. Vaccine *34*, 5815–5818. https://doi.org/10.1016/j.vaccine.2016.08.051.

110. Quinn, K.M., Zak, D.E., Costa, A., Yamamoto, A., Kastenmuller, K., Hill, B.J., Lynn, G.M., Darrah, P.A., Lindsay, R.W., Wang, L., and Cheng, C. (2015). Antigen expression determines adenoviral vaccine potency independent of IFN and STING signaling. J. Clin. Invest. *125*, 1129–1146. https://doi.org/10.1172/JCI78280.

111. Cirelli, K.M., Carnathan, D.G., Nogal, B., Martin, J.T., Rodriguez, O.L., Upadhyay, A.A., Enemuo, C.A., Gebru, E.H., Choe, Y., Viviano, F., and Nakao, C. (2019). Slow delivery immunization enhances HIV neutralizing antibody and germinal center responses via modulation of immunodominance. Cell *177*, 1153–1171 e1128. https://doi.org/10.1016/j.cell.2019.04.012.

112. Sliepen, K., van Montfort, T., Melchers, M., Isik, G., and Sanders, R.W. (2015). Immunosilencing a highly immunogenic protein trimerization domain. J. Biol. Chem. *290*, 7436–7442. https://doi.org/10.1074/jbc.M114.620534.

113. Crank, M.C., Ruckwardt, T.J., Chen, M., Morabito, K.M., Phung, E., Costner, P.J., Holman, L.A., Hickman, S.P., Berkowitz, N.M., Gordon, I.J., and Yamshchikov, G.V. (2019). A proof of concept for structure-based vaccine design targeting RSV in humans. Science *365*, 505–509. https://doi.org/10.1126/science.aav9033.

114. Stewart-Jones, G.B., Thomas, P.V., Chen, M., Druz, A., Joyce, M.G., Kong, W.P., Sastry, M., Soto, C., Yang, Y., Zhang, B., and Chen, L. (2015). A cysteine zipper stabilizes a pre-fusion F glycoprotein vaccine for respiratory syncytial virus. PLoS One *10*, e0128779. https://doi.org/10.1371/journal.pone.0128779.

115. Smith, K., Garman, L., Wrammert, J., Zheng, N.Y., Capra, J.D., Ahmed, R., and Wilson, P.C. (2009). Rapid generation of fully human monoclonal antibodies specific to a vaccinating antigen. Nat. Protoc. *4*, 372–384. https://doi.org/10.1038/nprot.2009.3.

116. Wang, S., Taaffe, J., Parker, C., Solorzano, A., Cao, H., Garcia-Sastre, A., and Lu, S. (2006). Hemagglutinin (HA) proteins from H1 and H3 serotypes of influenza A viruses require different antigen designs for the induction of optimal protective antibody responses as studied by codon-optimized HA DNA vaccines. J. Virol. *80*, 11628–11637. https://doi.org/10.1128/JVI.01065-06.

117. Dicks, M.D., Spencer, A.J., Edwards, N.J., Wadell, G., Bojang, K., Gilbert, S.C., Hill, A.V., and Cottingham, M.G. (2012). A novel chimpanzee adenovirus vector with low human seroprevalence: improved systems for vector derivation and comparative immunogenicity. PLoS One *7*, e40385. https://doi.org/10.1371/journal.pone.0040385.

118. Burke, D.F., and Smith, D.J. (2014). A recommended numbering scheme for influenza A HA subtypes. PLoS One *9*, e112302. https://doi.org/10.1371/journal.pone.0112302.

119. Reed, L.J., and Muench, H. (1938). A simple method of estimating fifty per cent endpoints. Am. J. Epidemiol. *27*, 493–497. https://doi.org/10.1093/oxfordjournals.aje.a118408.